ALMA MATER STUDIORUM - UNIVERSITÀ DI BOLOGNA

SCUOLA DI INGEGNERIA E ARCHITETTURA

DIPARTIMENTO DI INGEGNERIA CIVILE, CHIMICA, AMBIENTALE E DEI MATERIALI

CORSO DI LAUREA IN CIVIL ENGINEERING

TESI DI LAUREA

in

Advanced Design of Structures

Non-Linear Analysis and Design of Cable Systems in Suspension Bridges

CANDIDATO:

Riccardo Soli

RELATORE:

Prof. Stefano Silvestri

CORRELATORE:

Prof. Peter Ansourian

Anno Accademico 2016/2017

Sessione III

Summary

The scope of the presented research project is to provide a reliable guideline for the preliminary design of cable supported bridges. In order to pursue this objective, a thorough literature research has been conducted in the first phase of the project. This has been of relevant importance for the understanding of the subject and further implementation of the case study: the design of a suspension bridge model in Strand7.

The conducted research has shown that there is not a unique book to which engineers may refer in order to conduct the type of analysis presented in this project. Therefore, the proposed guideline has been created on the basis of multiple text books.

Further analyses have been conducted in order to evaluate the accuracy of theoretical-based results and software-based results. In particular the Steinman Modified Elastic Treatment has been applied to the case study and its results compared to those obtained on Strand7. The obtained results finally show that Steinman's Theory represents a quick and reliable method to be adopted for preliminary design purposes as its results are in line with Strand7 results.

Index

1. Introduction

Cable supported bridges are generally subdivided in two main categories depending on the asset of their cable system:

- Suspension Bridges, where the stiffening girder is connected to the main parabolic cables by means of vertical or inclined hangers;
- Cable-Stayed Bridges, where the stiffening girder is directly connected to the pylons by means of straight or quasi-straight cables.

The two typologies are shown in Figure 1.1 below.

Figure 1.1: Golden Gate Bridge (San Francisco, US) and Millau Viaduct (Creissels, France).

The non-linearity of the problem comes from the sag of the cables which provokes a non-constant tension along the cables' length. It is generally simpler to identify the sag in suspension bridges and more difficult in cable-stayed bridges due to different sag ratios adopted in practice. However, Figure 1.2 below shows the presence of sag in cable-stayed bridges:

Figure 1.2: Particular view of a cable-stayed bridge showing the sag of stay cables.

The conducted research is aimed to the determination of preliminary design guidelines for cable supported bridges, with a particular focus on suspension bridges. The common literature shows that the behaviour of stay cables can be generally approximated and related to that of straight cables with the adoption of some precautions. This has led to a greater personal interest in the behaviour of suspension bridges and it is therefore the reason why the case study reported in Chapter 3 refers to this type of structure.

First step of this project is the analysis of the main theories developed through history for cable supported bridges (Chapter 2), in order to gain the proper knowledge required for the implementation of the case study. As it is explained in Chapter 2, the ongoing development of the theories for cable supported bridges has led to numerical solutions that were once hard to be applied by structural engineers, who did not have the availability of softwares like Strand7 as we do today. Simplified theories were thus developed for practical purposes and this research will investigate the accuracy of one of these by comparing its results with those obtained on Strand7.

Chapter 3 reports the case study: the preliminary design of a suspension bridge and the creation of the Strand7 model to be adopted for further analyses. The reported guideline is the result of a research conducted on different text books and can be also applied to suspension bridges having different geometric characteristics to those adopted in this study. The design guidelines are particularly focussed on the cable system whilst the bridge's girder has been modelled on Strand7 according to common practice knowledge.
Moreover, Chapter 3 includes a comparison between the results obtained on Strand7 and those given by the application of the Steinman's Modified Elastic Treatment to the case study. The obtained results prove the reliability of Steinman's Theory and therefore make it a reliable tool to be adopted for the evaluation of the effect of Live Loads on the cable system.
Finally, an analysis of the effect of the side spans' length on the design of the suspension bridge has been conducted by the creation of a second model on Strand7.

2. Literature Review

2.1. Structural Behaviour of Cables

The non-linearity of cable systems due to the change in sag and axial tension represents a fundamental problem in the analysis of cable structures. Therefore the first thing that has to be analysed is the shape that a freely suspended cable would take when loaded by its own weight.

For obvious reasons the complete calculations for the determination of the cable's shape and tensions are not reported, as they can easily be found in many books and to which the following paragraphs are referred. The catenary problem was solved by J. Bernoulli at the end of the seventeenth century, whilst the solution to the parabolic curve was first proposed by N. Fuss at the end of the eighteenth century. Both solutions are collected in "The Theory of Suspension Bridges" (Pugsley 1968), and presented below.

2.1.1. Catenary Curve

The cable is assumed to be:

- Perfectly flexible: the cable carries any load by means of tension directed along its length;
- Inextensible;
- Uniform: weight per unit length (w') is constant along the cable.

Under these assumptions, the shape that the cable takes when suspended between two fixed nodes is known as "catenary".

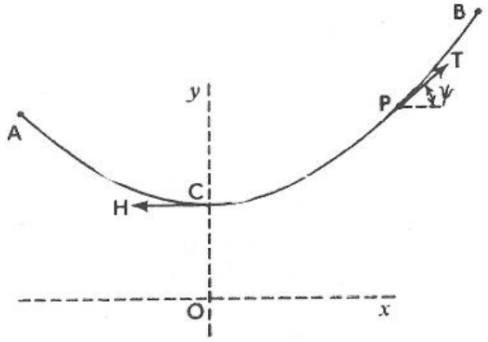

Figure 2.1: Catenary Curve (Pugsley 1968).

This problem has been solved by starting from Equilibrium equations:

$$(1) \quad \begin{cases} T\cos(\psi) = H \\ T\sin(\psi) = w's \end{cases}$$

where T is the tension at any point of the cable, and H is the tension in the cable at point C.

As outputs it is possible to obtain the “Cartesian Equation of the Catenary”:

$$(2)\quad y = c \cdot \cosh\left(\frac{x}{c}\right)$$

where “c” is the “parameter of the catenary”, which can be obtained by using tables of hyperbolic functions.

Moreover, the tension in the cable is expressed by the following:

$$(3)\quad T = w' \cdot y$$

and its horizontal component is expressed as:

$$(4)\quad \begin{cases} H = w' \cdot \left[s \cdot \cot(\psi) \right] \\ H = w' \cdot c \end{cases}$$

The following observation can be made upon the obtained results:

- The horizontal component of the cable’s tension, shown in equation 4, is constant;
- The vertical component of the cable’s tension is expressed at any point of the cable as:

$$(5)\quad w' \cdot s = w' \cdot c \sinh\frac{x}{c}$$

2.1.2. Parabolic Curve

The cable is assumed to be:

- Perfectly flexible: the cable carries any load by means of tension directed along its length;
- Inextensible.

The third assumption though is different from the one considered in the catenary formulation, as it refers to a practical situation in which the total dead weight of the structure is uniformly distributed along the span of the bridge, not along the cable. Therefore the third assumption is:

- Weight per unit length (w) is uniformly distributed along the span.

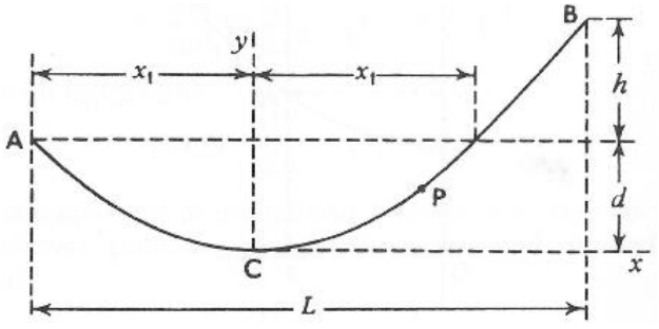

Figure 2.2: Parabolic Curve (Pugsley 1968).

This problem has been solved by starting from Equilibrium equations:

$$(6)\quad \begin{cases} T\cos(\psi) = H \\ T\sin(\psi) = w \cdot s \end{cases}$$

where T is the tension at any point of the cable, and H is the tension in the cable at point C. The "Cartesian Equation of the Parabolic Cable" obtained is:

$$(7)\quad y = \frac{1}{2}\frac{w}{H} \cdot x^2$$

For the practical case of parabolic cable freely suspended between two nodes A and B at the same level, the tension in the cable T can be expressed as:

$$(8)\quad T = H \cdot \sqrt{1 + \frac{64 d^2 x^2}{\frac{L}{4}}}$$

with horizontal component H equal to:

$$(9)\quad H = \frac{wL^2}{8d}$$

A useful result that this analysis provides in practical terms is the length of the sagging cable "l". Assuming small ratios of d/L this length can be expressed as:

$$(10)\quad l = L \cdot \left[1 + \frac{8}{3}\left(\frac{d}{L} \right)^2 \right]$$

2.1.3. Cable with Inclined Chord

This study case is particularly useful for the analysis of cable-stayed bridges and the side span cables of suspension bridges. The complete calculations for this case are reported in "Statically Indeterminate Structures" (Maugh 1964) but for practical reasons only the main results are listed in this review, and were taken from "Construction and Design of Cable Stayed Bridges" (Walter Podolny 1976). When considering the condition represented in Figure A2.1 (reported in the Appendix), the relevant results are:

- Horizontal component of cable stress (H):

$$(11)\quad H = \frac{wL^2}{8f'}$$

- Maximum tension stress in the cable (T_{max}):

$$(12)\quad T_{\max} = H\left[1+\left(\frac{h}{L}+4n\right)^2\right]^{1/2}$$

- Vertical components of cable stress:

$$(13)\quad V_r = \frac{Hh}{L}+\frac{wL}{2}$$

- Cable length:

$$(14)\quad S \simeq L\sec\vartheta\cdot\left(1+\frac{8n^2}{3\sec^4\vartheta}\right)$$

- Cable elongation due to cable tension stress:

$$(15)\quad \Delta S \simeq \frac{HL}{AE}\sec\vartheta\cdot\left(1+\frac{16n^2}{3\sec^4\vartheta}\right)$$

- Sagging cable's (y) coordinates from the inclined chord:

$$(16)\quad \mathrm{y} = \frac{4f'}{L^2}\left(Lx-x^2\right)$$

It must be noted that in the practical analysis of cable-stayed bridges the inclined cable is usually assumed as a straight line. Podolny investigated the percentage error of cable tension due to this approximation and provided the results plotted in Figure A2.2 (reported in the Appendix) (Walter Podolny 1976). As it can be noticed from the plot, when the sag ratio is in the range 1:30 - 1:100, the error varies from 4% to 12% depending on the chord inclination.

2.1.4. Comparison of Cable Shapes

After the study of the two shapes that have just been analysed, D. Gilbert developed some calculations for the case of "The Catenary of Uniform Strength", in which he investigated how cables having sectional area varying proportionally to their tension would behave. However, since the cables usually adopted in practice for the construction of suspension bridges have a uniform cross-sectional area, the results of this analysis will not be reported (Pugsley 1968).

Now that the two shapes that a cable would take under its own weight are known, it must be understood which model should be chosen for practical interest. Theoretically, the weight per unit length of a freely suspended cable would be constant along its length, therefore suggesting that the catenary curve is the most precise representation of a cable's shape.

However, in practice, the stiffening girder on which the roadway is constructed is so hung to the cables by means of suspension rods that when the structure is completed and the temporary sustaining platforms removed, the cables will take a parabolic shape. It can therefore be stated that for practical purposes a parabolic form of the cable could be considered.

Support to this statement was not only given in Sir A. Pugsley's book "The Theory of Suspension Bridges", but can be also found in "Construction and Design of Cable Stayed Bridges", a work by W. Podolny and J.B. Scalzi published in 1976 (Pugsley 1968; Walter Podolny 1976).

A logarithmic plot of the catenary and parabolic curves based on the sag ratio (n):

$$(17)\quad n = f / l \qquad \text{and} \qquad (18)\quad m = 2a / l$$

shows that the catenary curve and the parabolic curve diverge at a sag ratio of 0.15 (Walter Podolny 1976):

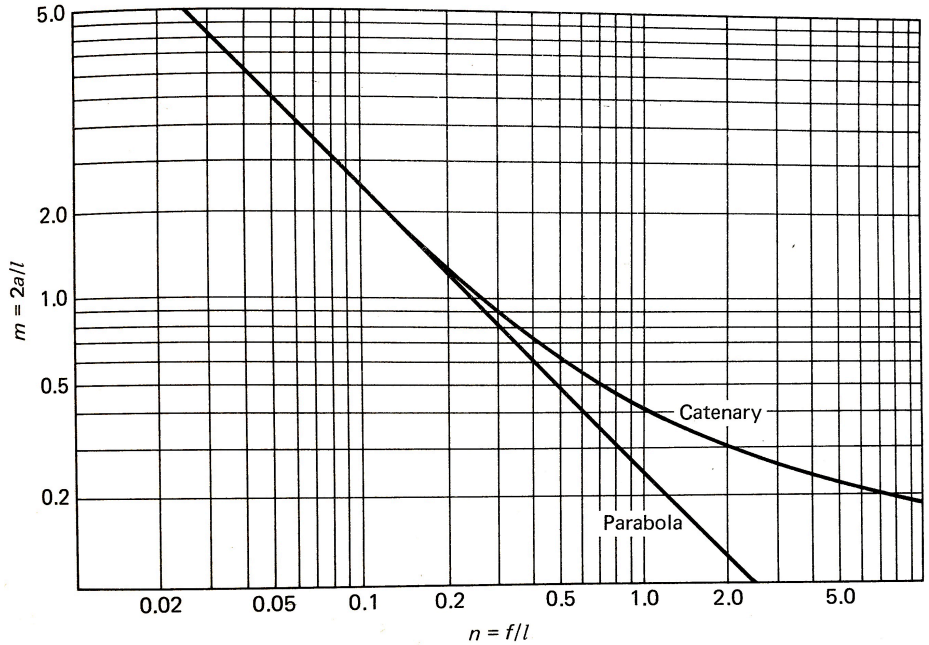

Figure 2.3: Catenary versus parabola (Walter Podolny 1976).

where (f) and (a) are defined in Figure A2.3 (reported in the Appendix) (Walter Podolny 1976).

Thus it can be stated that for sag ratios smaller or equal to 0.15, the approximation of the catenary curve with a parabolic curve represents a reasonable choice (Pugsley, 1968).

However, a practical example will be analysed in chapter 3 in order to determine the accuracy of the reported results.

2.1.5. Final Considerations

The analysis of the proposed results suggests that a parabolic curve can be adopted in future analysis as the sag ratios usually adopted in practice are comparable to 0.15.

It must be noted that the assumption of "inextensible cable" was considered in both the catenary and parabolic curve solutions (paragraphs 2.1.1 and 2.1.2). This assumption of course simplifies the analysis of cable structures but does not accurately represents reality. The first solution to the "Elastic Catenary" problem was given by Routh in 1891 (Routh 1891) but the result was too difficult to be applied in practical cases.

However, a simpler solution based on the parabolic curve was provided by Rankine in 1858 (Rankine 1858). Assuming that

- The cable is extensible;
- The span L remains constant;

the change of dip Δd can be calculated from the following system:

$$(19)\quad \begin{cases} \Delta l = \dfrac{16 \cdot d}{15 \cdot l}\left[5 - 24\left(\dfrac{d}{L}\right)^2\right]\Delta d \\ \Delta l = \dfrac{H \cdot l}{AE}\left[1 + \dfrac{16}{3}\left(\dfrac{d}{L}\right)^2\right] \end{cases}$$

Once again this result is based on the assumption of constant span (L), which can not be ensured in practical cases as it depends from the bridge's pylons. During the design phase, further considerations will thus have to be made to account for certain effects due to simplifications.

The second assumption on which we may focus is the one that considers the cable as "perfectly flexible", thus neglecting the flexural rigidity that a real cable would have. An interesting analysis regarding the influence of flexural rigidity was conducted by H.M. Irvine and reported in his book "Cable Structures". In particular, the following expression for the dip of a cable's profile below the inclined chord is provided:

$$(20)\quad z = \frac{x(1-x)}{2} - \frac{1}{\gamma^2}\left(1 + \tanh\frac{\gamma}{2}\sinh\gamma x - \cosh\gamma x\right)$$

where (z) and (x) are the non-dimensional coordinates as shown in Figure A2.4 (reported in the Appendix). The parameter (γ):

$$(21) \quad \gamma = \sqrt{\frac{H \cdot l^2}{EI}}$$

represents the relative contribution to the cable's behaviour as if it were treated as a perfectly flexible cable or as a beam element. As it is explained in Irvine's analysis, the value of γ is usually large for the majority of cable problems (order of 10^3) and therefore the effect of flexural rigidity can be neglected. However, when concentrated loads are applied to the cable and rapid changes in curvature are unavoidable, the effect of flexural rigidity increases (Irvine 1981).

2.2. Structural Behaviour of Cables under Applied Loads

Once that the shape of a freely suspended cable is known, further analysis of the deformed shape that it would assume under applied loads can be conducted. The capability of a cable to resist deformation by means of its own weight is of fundamental interest in the analysis of suspension bridges. Rankine payed particular attention to this aspect in the Theory he published in 1858 (Rankine 1858), and the results presented in the following paragraphs were also inspired to some unsigned articles in the "Civil Engineering and Architects' Journal" for November and December 1860 (Pugsley 1968). As for the previous paragraph, calculation won't be reported but reference will be made to relevant assumptions and results (Pugsley 1968).

2.2.1. Single Concentrated Load

Assumptions:

- Nodes A and B are positioned at the same level;
- The cable is subject to a load (w) which is uniformly distributed along the span L, and includes the self-weight;
- Cable hangs in a parabolic shape (of which point C is the vertex);
- The cable is inextensible.

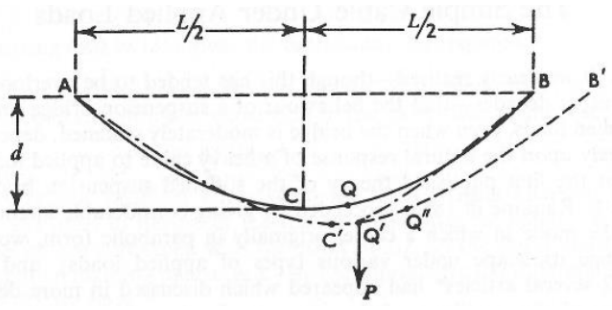

Figure 2.4: Parabolic cable under the action of a concentrated load (Pugsley 1968).

In the undeformed configuration the equations expressing the parabolic shape and the tension (H) in the cable at point (C) are:

$$(1)\quad y = \frac{1}{2}\frac{w}{H}\cdot x^2 \qquad ; \qquad (2)\quad H = \frac{wL^2}{8d}$$

as already reported in paragraph 2.1.2., by formulas (7) and (9).

When a force P is applied at Q, the vertex of the parabolic cable will shift to its new position (C'), and the tension at this point will be:

$$(3)\quad \left(H + h\right)$$

where (h) is the tension increment due to P.

The equation used to express the shape of the portion (A-Q') of the cable will therefore be:

$$(4)\quad \mathrm{y}_1 = \frac{w}{2\left(H + h\right)}x_1^2$$

where the parameters x_1 and y_1 are referring to the new vertex (C'). The position of this new vertex is obtained by the equilibrium equations of the vertical forces and bending moment. In particular, the coordinates x_0 and y_0 of point (C') measured from the initial vertex (C) are:

$$(5)\quad \begin{cases} x_0 = \dfrac{P}{W}\left(\dfrac{1}{2} - r\right) \\ y_0 = d - \dfrac{wL^2}{8\left(H + h\right)}\cdot\left[1 + \dfrac{P}{wL}\left(1 - 2r\right)\right]^2 \end{cases}$$

where (r = x/L) is also used to determine how the concentrated load is shared by the vertical reactions:

$$(6)\quad \begin{cases} V_A = \dfrac{wL}{2} + P\left(\dfrac{1}{2} - r\right) \\ V_B = \dfrac{wL}{2} + P\left(\dfrac{1}{2} + r\right) \end{cases}$$

In order to define the tension increment due to P (h) a further assumption has to be made:

- The extension of the cable due to (h) is negligible.

The result provided therefore is:

$$(7)\quad h = \frac{3}{2}H\frac{P}{wL}\left(1 - 4r^2\right)$$

Further interesting considerations regarding the case of "Single Concentrated Load" are presented in (Pugsley 1968):

A. Vertical Deflections Under Concentrated Load

The relation expressing the vertical deflection at the loaded point (Q), where (x=rL), is:

$$(8)\quad \upsilon_Q = -\frac{P}{wL}\cdot d\cdot\frac{\left(1+12r^2\right)\left(1-4r^2\right)}{2+\frac{3P}{wL}\left(1-4r^2\right)}$$

where (r) represents the distance between the point (Q) where the force is applied and the parabola's vertex (C) . A plot of the deflection (υ) for different values of (r) and (P/wL) is also provided in Figure A2.5 (reported in the Appendix).

Based on the results of Figure A2.5, a relevant consideration can be made: as the value of (P) increases the cable becomes stiffer. However, if it is assumed that the values of (P/wL) are small, formula (8) can be approximated and linearised as it follows:

$$(9)\quad \upsilon_Q = -\frac{P}{2wL}\cdot d\cdot\left(1+12r^2\right)\left(1-4r^2\right)$$

By differentiating formula (9) it can be noted that that the maximum deflection is obtained for:

$$(10)\quad r=\frac{1}{\sqrt{12}}$$

This means that the maximum deflection is obtained when the concentrated load (P) is applied at a distance of (0.29L) from the centre of the span, and it is equal to:

$$(11)\quad \upsilon_Q = -\frac{2}{3}\frac{P}{wL}d$$

If it is assumed that the concentrated load is applied at the centre of the span (r=0), the deflection will be:

$$(12)\quad \upsilon_Q = -\frac{1}{2}\frac{P}{wL}d$$

B. Influence Coefficients for Deflection

The author (Sir A. Pugsley) provides a table of flexibility coefficients for vertical deflections due to vertical concentrated loads. For the purpose of this analysis the cable was subdivided by means of nine points equally distributed along the span. By considering the following assumptions (Pugsley 1968):

- The concentrated load is small compared to the weight of the cable and deck (P/wL=0.1)
- The principle of superposition applies
- The ratio d/L (dip to span) is small (0.1 approximately)

and by making use of formula (9), a set of flexibility coefficients can be calculated.

These flexibility coefficients are reported in Figure A2.6 (in the Appendix) and used to plot the influence lines for the analysis of cable's deflection subject to a system of concentrated loads. In Figure 2.5 below, a plot of the influence lines for concentrated loads applied to stations 1 (in blue colour) to 5 (in red colour) are reported (the data were plotted using Excel):

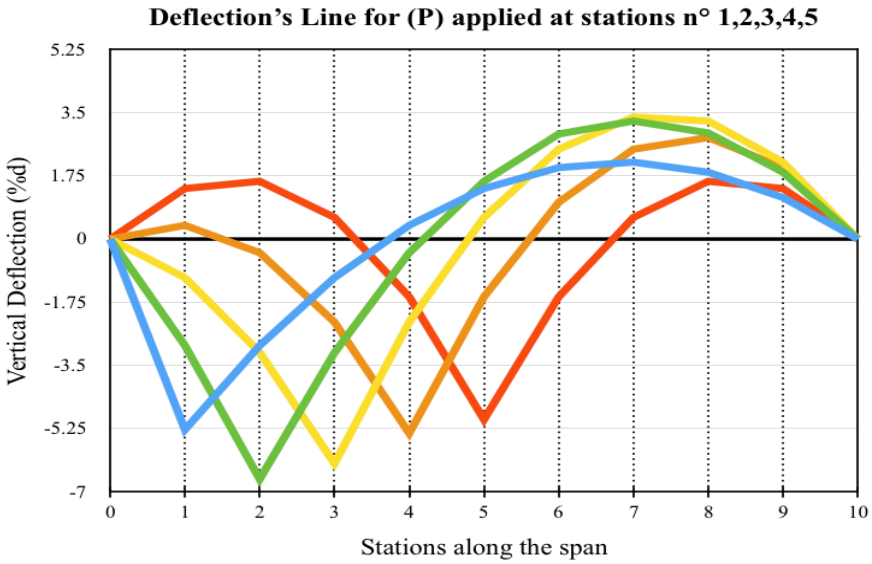

Figure 2.5: Deflection's lines for P applied at station points 1 to 5.

The horizontal origin axis represents the initial parabolic shape. The peak value for a given station (i) is of course obtained when the load (P) is applied at station (i). The maximum vertical downward deflection is obtained when (P) is applied at station 2 (green line).

2.2.2. A Short Distributed Load Centrally Placed

The assumptions to be considered are the same as those already reported in paragraph (2.2.1). The distributed load (p) is applied on a length of [(1-2n)L], and the self weight (w) is considered as well.

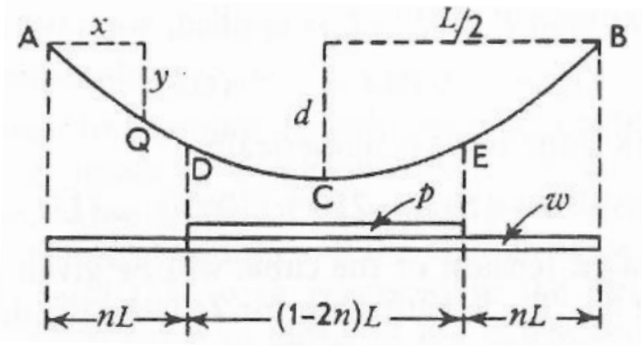

Figure 2.6: Parabolic cable under the action of a load centrally placed (p) (Pugsley 1968).

Under these conditions the following results are obtained (Pugsley 1968):

- Vertical reactions:

$$(13)\quad V_A = V_B = \frac{wL}{2} + \frac{(1-2n)\,pL}{2}$$

- Equation of the parabolic arch AD (same shape assumed by arch EB):

$$(14)\quad y_{AD} = \frac{wx(L-x) + pLx(1-2n)}{2H}$$

- Equation of the parabolic arch DE:

$$(15)\qquad y_{DE} = \frac{(p+w)(L-x)x - pn^2L^2}{2H}$$

- Final dip (D) at the centre of the span, expressed as a function of the initial dip (d) due to self weight only:

$$(16)\quad D = d \cdot \frac{\left[\left(\frac{p}{w}+1\right) - 4n^2\frac{p}{w}\right]}{\sqrt{\left(\frac{p}{w}+1\right)^2 - 4n^2\frac{p^2}{w^2}(3-4n) - 4n^2\frac{p}{w}(3-2n)}}$$

- The tension in the cable for (x=L/2):

$$(17)\quad H = \frac{L^2}{8D}\left[(p+w) - 4n^2p\right]$$

2.2.3. A Short Distributed Load at One End of the Span

The assumptions to be considered are the same as those already reported in paragraph (2.2.1). In this case the distributed load (p) is applied at one end of the span as shown in the following figure (Pugsley 1968):

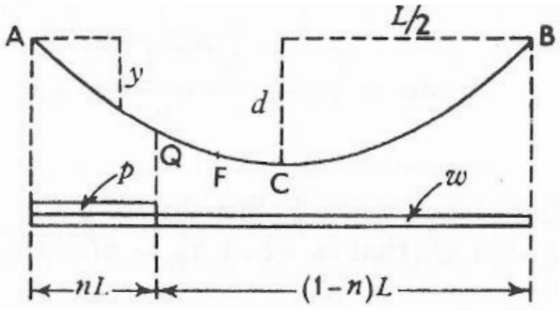

Figure 2.7: Parabolic cable under the action of a load (p) placed at one end of the span (Pugsley 1968).

Under these conditions the following results are obtained:

- Equation of the parabolic arch AQ, subject to the distributed loads (w) and (p):

$$(18)\quad y=\frac{4d}{L^2}\cdot\frac{\left(\frac{p}{w}+1\right)x\left(L-x\right)-\left[\left(\frac{p}{w}\right)Lx\left(1-n\right)^2\right]}{\sqrt{1+2\left(\frac{p}{w}\right)\left(3-2n\right)n^2+\left(\frac{p}{w}\right)^2 n^3\left(4-3n\right)}}$$

- Equation of the parabolic arch QB, subject to the distributed load (w):

$$(19)\quad y=\frac{4d}{L^2}\cdot\frac{\left(\frac{p}{w}n^2L+x\right)\left(L-x\right)}{\sqrt{1+2\left(\frac{p}{w}\right)\left(3-2n\right)n^2+\left(\frac{p}{w}\right)^2 n^3\left(4-3n\right)}}$$

- The tension in the cable at the centre of the span:

$$(20)\quad H=\frac{wL^2}{8d}\sqrt{1+2\left(\frac{p}{w}\right)\left(3-2n\right)n^2+\left(\frac{p}{w}\right)^2 n^3\left(4-3n\right)}$$

In this case it will result more interesting to investigate the change of dip at a point F (as shown in the previous figure), rather than at the centre of the span, as it will become the lowest point under the action of (w) and (p). In particular, let x_F and y_F be the coordinates of point F:

- if $\left(x_F > nL\right) \Rightarrow$ F occurs in the arch QB $\Rightarrow$ $(21)\quad x_F=\frac{L}{2}\left(1-\frac{p}{w}n^2\right)$

- if $\left(x_F < nL\right) \Rightarrow$ F occurs in the arch AQ $\Rightarrow$ $(22)\quad x_F=\frac{L}{2}\cdot\frac{1+\frac{p}{w}n\left(2-n\right)}{1+\left(p/w\right)}$

By substituting (21) in (19) or (22) in (18), the change of dip at point F can be obtained.

2.2.4. Final Considerations

As it can be noted from the results presented in the previous paragraphs, the cable's flexural rigidity is not taken into account. It is therefore interesting to understand how this aspect could affect the analysis of cable structures. As we will see in the following paragraphs, the effect of the flexural rigidity has been simplified in the earlier theories for the analysis of suspension bridges, and has only been considered at later stages.

2.3. Analysis of the Theories for Suspension Bridges

A brief analysis of the main theories that were developed for suspension bridges will be conducted in this chapter. The focus will be on the main assumptions on which these theories are based, on the obtained results, their evolution and limitations.

2.3.1. The Rankine Theory (1858)

This is considered as the first proper theory of suspension bridges and was firstly published in 1858 by W.J.M. Rankine in "A manual of Applied Mechanics" (Rankine 1858). The proposed theory has also been included in other textbooks such as "The Analysis of Engineering Structures" (A. J. S. Pippard 1968) and "The Theory of Suspension Bridges" (Pugsley 1968). Rankine's purpose was to demonstrate that there was no need to construct girders so stiff that they could bear their own weight, otherwise the role of the cable would have been pointless. The considered scheme will be the following:

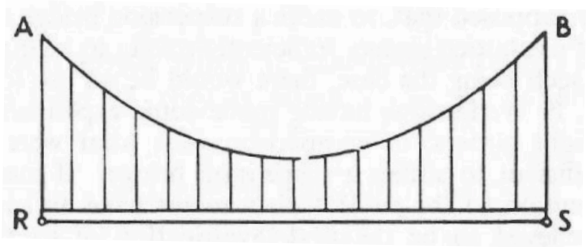

Figure 2.8: Single span scheme (Pugsley 1968).

where points A, B, R and S are fixed.

- **<u>Assumptions on which the Rankine's Theory is based</u>**
    1. The cable takes a parabolic shape under the action of the total dead load on the bridge, and the stiffening girder would be unstressed
    2. The stiffening girder redistributes any live loading so that the cable will be subject to a uniformly distributed load along its span;
    3. The uniformly distributed upward pull that the cable is transmitting to the stiffening girder, is equal to the total live load divided by the span (L).

Assumption 2 is implicitly stating that the girder's stiffness is relatively high.

The results reported in the following paragraphs were obtained by means of equilibrium only, with no regard to the displacement's compatibility (A. J. S. Pippard 1968; Pugsley 1968).

A. <u>Two-pinned Stiffening Girder with a Single Concentrated Load</u>

A load P is applied at a point Q, the upward pull (q) will therefore be:

$$(1) \quad q = \frac{P}{L}$$

By applying equilibrium the vertical reactions can be found:

$$(2) \quad V_R = -V_S = \frac{P}{L}\left(\frac{L}{2} - x\right)$$

The Bending Moment (B.M.) and Shear Force's (S.F.) diagrams are provided in Figure A2.7 (reported in the Appendix). For the Bending Moment diagram, the upward pull (q) will result in a parabolic curved diagram, whilst the concentrated load (P) results in a triangular diagram. The obtained values are:

- Maximum value of the bending moment: (3) $M_Q = -\frac{Px\left(L-x\right)}{2L}$
- When (P) is applied at midspan: $x = L/2 \Rightarrow$ (4) $M_Q = -\frac{PL}{8}$

The increase in the horizontal component of the tension in the cable is:

$$(5) \quad h = \frac{qL^2}{8d} = \frac{PL}{8d}$$

and due to Assumption 3 the value of (h) is constant and does not depend on the point of application of the force (P).

It is also interesting to show how the bending moment (4) and the cable's horizontal component of the tension (5) would change when considering a simply supported girder in absence of the cable, and a cable in absence of the girder. For a concentrated load (P) applied at midspan the following results can be compared:

	Suspension Bridge	**Girder**	**Effect of the Cable**
M_Q	$-\frac{PL}{8}$	$-\frac{PL}{4}$	The presence of the cable therefore halves the B.M. at midspan

	Suspension Bridge	**Cable**	**Effect of the Girder**
h	$\frac{PL}{8d}$	$\frac{3PL}{16d}$	The presence of the girder reduces (h) by 50%

Rankine also plotted the influence lines for bending moment and shear force in the stiffening girder, reported in Figure A2.8 (in the Appendix).

B. Two-pinned Stiffening Girder with a Uniform Load

By referring to the previous figure showing the influence lines for a concentrated load, it can be deducted that the maximum bending moment on the girder will occur for a load (p) of length (L/2) placed on top of the negative triangle. In particular, this bending moment can be calculated as the area of that triangle as (Pugsley 1968):

$$(6) \quad M_Z = -\frac{1}{8} pL^2 \left(1-n\right) n$$

The maximum value of the bending moment is obtained for ($n = L/2$), thus when point (Z) corresponds to point (C):

$$(7) \quad M_C = -\frac{pL^2}{32}$$

This value can be compared to the bending moment value in the girder in case that the cable was absent:

	Suspension Bridge	**Girder**	**Effect of the Cable**
M_C	$-\frac{pL^2}{32}$	$-\frac{pL^2}{8}$	The presence of the cable reduces the B.M. at midspan to a quarter of the value that a simply supported beam would have

The effect of the cable would suggest that the required bending strength of the girder should be one quarter (1/4) of the one that a simply supported beam would have under the same applied load. Further calculations where done by Rankine for different load distributions and these led to the following result: the girder of a suspension bridge should have a bending strength which is approximately seven times smaller than that of a simple beam in order to carry the same loading (Pugsley 1968).

C. Three-pinned Stiffening Girder with a Single Concentrated Load

In this case the insertion of the central hinge has three main effects, that have to be compared to the results reported in case "*A. Two-pinned Stiffening Girder with a Single Concentrated Load*":

- The upward pull is now a function of (x):

$$(8) \quad q = \frac{4Px}{L^2}$$

- The horizontal component of tension in the cable will therefore be:

$$(9) \quad h = \frac{qL^2}{8d} = \frac{Px}{2d}$$

- A greater part of the applied load is carried by the cable. In fact the value of (h) when (P) is applied at the centre of the span is:

$$(10) \quad h = \frac{PL}{4d}$$

which is twice the value that was obtained for the two-pinned girder.

D. <u>Three-pinned Stiffening Girder with a Uniform Load</u>

In this case the insertion of the central hinge has one main effect, that have to be compared to the results reported in case "B. *Two-pinned Stiffening Girder with a Uniform Load*":

- The critical length to be loaded in order to obtain the maximum bending moment is smaller ($0.395L$ instead of $L/2$) and its value is approximately 40% smaller.

2.3.2. The Elastic Theory (19th century)

This theory was developed throughout the nineteenth century thanks to the application of the "Theory of Arches" by Navier (Résumé des Leçons données à l'Ecole des Ponds et Chaussées, 1826) and to later works conducted by Castigliano (Castigliano 1879). The well known "The Analysis of Engineering Structures" (A. J. S. Pippard 1968) was the first English book reporting this theory.

- ***<u>Assumptions on which the Elastic Theory is based</u>***

The firs two assumptions are the same as those proposed in Rankine's Theory:

1. The cable takes a parabolic shape under the action of the total dead load on the bridge;
2. The stiffening girder is unstressed;

The element of innovation stands in the third assumption:

3. The uniformly distributed load (q) acting on the cable mainly depends on four elements:
   I. Girder's stiffness (in bending)
   II. Cables' stiffness (in tension)
   III. Suspension rods' stiffness
   IV. Towers' stiffness

As it has already been discussed, cable's behaviour under applied loads is non-linear. However, due to the small displacement's values typically involved in practice, the Hooke's

Law is considered to be valid, and a linear strain-energy treatment can be adopted for the determination of (q) (Pugsley 1968).

Study Case: The Two-pinned Girder of a Single Span Bridge with a Single Concentrated Load

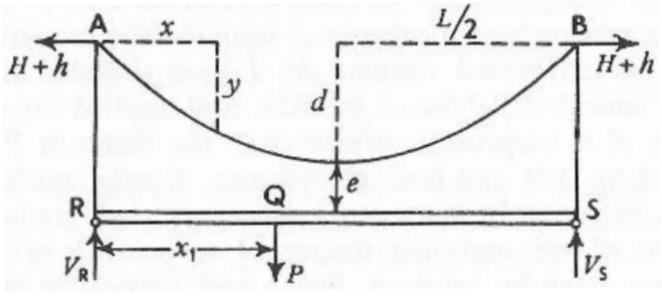

Figure 2.9: Adopted scheme for a two-pinned girder with concentrated load (P) (Pugsley 1968).

The bending moment at a certain section (x) can be expressed as the sum of two contributions expressing the effect of (P) and (q):

$$(1) \quad M = \mu + hy$$

where:

$$(2) \quad \begin{cases} \mu = \dfrac{Px\left(L - x_1\right)}{L} \\ h = \dfrac{qL^2}{8d} \end{cases}$$

Formula (1) is based on the assumption that the girder deflection "υ" is negligible compared to the ordinates "y" of the initial cable shape. This particular simplification will be reviewed in the Deflection Theory.

By calculating the total strain energy due to the four elements reported in Assumption 3 and equating it to zero, the increase in the horizontal component of tension (h) due to (P) can be calculated:

$$(3) \quad h = \frac{\dfrac{Px_1 d}{3EI}\left[L - \dfrac{x_1^2}{L^2}\left(2L - x_1\right)\right]}{\dfrac{8Ld^2}{15EI} + \dfrac{cL}{AE} + \dfrac{64d^2}{L^3 aE}\left(e + \dfrac{d}{3}\right) + \dfrac{32d^2\left(e+d\right)}{A_2 EL}}$$

where "c" is a parameter proportional to (d^2 / L^2) and "a" is the rod's sectional area per unit length of the span. The terms in the denominator of formula (3) are referred to the four elements considered, following their order:

I. Stiffening Girder, contributing for 95%

II. Cable, contributing for 4-5%

III. Suspension rods, contributing for a fraction of 1%

IV. Towers, contributing for a fraction of 1%

Formula (3) can thus be approximated to:

$$(4)\quad h = \frac{\frac{Px_1 d}{3EI}\left[L - \frac{x_1^2}{L^2}\left(2L - x_1\right)\right]}{\frac{8Ld^2}{15EI} + \frac{cL}{AE}}$$

The bending moment in every point of the beam can be obtained by substituting (4) in (1). Moreover, the value of the loading (q) acting on suspension rods can be obtained by substituting (4) in the following:

$$(5)\quad q = \frac{8hd}{L^2}$$

It is now interesting to analyse the consequences of the adopted simplification to obtain formula (4). If we assume that the second term of the denominator is negligible (contributing for 4-5% only), then the expression of "h" will become independent of the stiffness EI. For the case of (P) applied at the centre of the span (x=L/2) we'll have:

$$(6)\quad h_{Elastic} = \frac{25}{128}\frac{PL}{d}$$

This further assumption corresponds to considering the cable as inextensible, thus stepping back to the same conditions on which the Rankine's theory was based. We can therefore compare (6) with the expression of (h) provided by Rankine and reported in paragraph 2.3.1 - formula (5):

$$(5 - 2.3.1)\quad h_{Rankine} = \frac{PL}{8d}$$

We can deduct that the increase in the horizontal component due to (P) applied at midspan is larger when calculated using the Elastic Theory:

$$(8)\quad h_{Elastic} = \frac{25}{16}\cdot h_{Rankine} \quad \left(\simeq 1.56 \cdot h_{Rankine}\right)$$

The influence lines for bending moment and shear forces are plotted in terms of $\left(\mu / y\right)$ and $\left(h\right)$ (refer to Figure A2.9 in the Appendix) by adjusting formula (1) into its new form:

$$(9)\quad M = \left(\frac{\mu}{y} + h\right) y$$

The value of the peak bending moment for this study case can be compared to the corresponding case analysed in Rankine's Theory. For a concentrated load (P) applied at point (Z), when (Z) is placed at the centre of the span, the maximum bending moment's value in the girder is:

$$(10)\quad M_{Elastic} = -\frac{7}{128} L$$

If we compare this result with the one obtained in paragraph 2.3.1 - formula (4):

$$(4 - 2.3.1)\quad M_{Q(Rankine)} = -\frac{PL}{8}$$

we can deduct that the Elastic Theory provides a lower value for the peak bending moment, in particular:

$$(12)\quad M_{Elastic} = \frac{7}{16} M_{Rankine} \quad \left(\simeq 0.44 \cdot M_{Rankine}\right)$$

2.3.3. The Deflection Theory (1888)

The Deflection Theory represents an advance of the Elastic Theory as it takes into consideration the effect of the girder's deflection (υ). When this is considered, the bending moment in the girder will be reduced and the girder's design will be affected as well.

The Theory was proposed by J. Melan in his book "Theorie der eisernen Bogenbrücken und der Hängebrücken, Handbuch der Ingenieurwissenschaften (1888)", and reported in many other textbooks (A. J. S. Pippard 1968; Pugsley 1968).

The starting point is the review of the bending moment expression provided by the Elastic Theory (formula 1 - paragraph 2.3.2), that is rewritten as:

$$(1)\quad M = \mu + hy + \left(H + h\right)\upsilon$$

where the deflection (υ) is taken into account. The theory then proceeds in the analysis of a single-span suspension bridge by means of differential equations. The analysis of course is non linear and may result quite difficult to be applied in the design phase of a real structure. Solutions for many loading cases have been obtained and collected in the books "A Practical Treatise on Suspension Bridges" and "Theory and Practice of Modern Framed Structures" (J.B. Johnson 1910; Steinman 1922).

In order to exploit the Deflection Theory for practical purposes, several simplified methods have been proposed:

- The Linearised Deflection Theory
- The Fourier Series Treatment of the Deflection Theory
- Approximate Methods of Analysis for Preliminary Design

A. The Linearised Deflection Theory

The linearised solution for Deflection Theory was proposed in 1894 by Godard (Godard 1894)) and subsequently adopted and reanalysed by H. Bleich (Bleich 1935). Bleich also plotted a graph in order to demonstrate that, for small values of the applied load (p) compared to the dead load (w), the Linearised Deflection Theory is more accurate than the Elastic Theory in providing the value of the girder's deflection (Figure A2.10 in the Appendix).

Sir A. Pugsley also included in his work three different methods to be developed on the Linearised Deflection Theory (Pugsley 1968):

- Tie Analogy Method
- Flexibility Coefficient Method (due to Pugsley himself)
- Energy Method (initiated by Timoshenko in 1930)

B. The Fourier Series Treatment of the Deflection Thoery

The use of series for treating the Deflection Theory was primarily adopted by Timoshenko in 1928 (Timoshenko 1928), then reanalysed by Southwell and Atkinson (R.J. Atkinson 1939).

In particular, Southwell developed the "Relaxation Method" for the design of suspension bridges. In his method, both the horizontal movements of the cable and the variable section of the stiffening girder were accounted.

C. Approximate Methods of Analysis for Preliminary Design

As the Deflection Theory improved, the methods of analysis for suspension bridges became more difficult due to their numerical approach. This led to the origin of three simplified methods for the application to practical cases that can be found in the work of Sir A. Pugsley (Pugsley 1968):

- *Steinman's Modified Elastic Treatment:* As its name suggests, this treatment is based on the Elastic Theory already reported in paragraph 2.3.2. As the Elastic Theory is reliable for short spanned bridges and stiff girders only, this method is based on the calculation of stiffness parameter that can be used to adapt the Elastic Theory's solutions to a wider

variety of suspension bridges. This method is reported in "A practical Treatise on Suspension Bridges" by D.B. Steinman (1929) and will be adopted further on in this research in order to test its accuracy.

- *Hardest and Wessman's Cable Treatment:* This method was proposed by Hardesty and Wessman in their work "The Preliminary Design of Suspension Bridges" (1939). This method focuses on a more accurate determination of the cable's deflection under applied loads. The idea of this treatment, is that the load pattern causing the maximum deflection in the cable, is also provoking peak values of the bending moment in the stiffening girder.
- *Elastic Foundation Analogy:* The solution to the Elastic Foundation's problem is adopted in the analysis of a suspension bridge. Particular attention is given to the bending moment and deflection of the stiffening girder and relevant results were obtained for practical application in the design phase.

2.3.4. Final Considerations

The table below provides a brief summary of the main limitations and improvements of the theories presented in paragraph 2.3.

Theory	Limitations	Improvements
Rankine	• Flexural stiffness of the girder considered as extremely high; • Displacement's compatibility neglected; • Reliable for span of 200/300 (m).	The stiffening girder does not need to be designed in order to sustain its entire weight.
Elastic	• The girder's deflection is neglected in the determination of the bending moment "M" (formula 1). Therefore the reducing effect that deflection would have on the bending moment is not taken into consideration; • The cable maintains its parabolic shape under the action of any applied load. In reality this shape would change accordingly with the load.	The load (q) acting on the cable accounts for the stiffness of four elements (cable, girder, rods and towers).
Deflection	Based on complicate numerical solutions, which therefore require approximation for practical design purposes.	Accounts for: • Girder's deflection • Horizontal movements of the cable • Variable girder's cross section

The evolution of these theories clarified that the primary bearing function in suspension bridges relied on cables. As a cause of this understanding, stiffening girders were built less stiff, lighter and their slenderness obviously increased. For instance, the span and longitudinal slenderness of some of the most famous suspension bridges are reported in the following chart:

Bridge	Span	Longitudinal Slenderness
Golden Gate	1260 m	1/168
Verrazzano	1298 m	1/180
Tacoma	853 m	1/350

However, the failure of the Tacoma Narrows Bridge revealed one of the key issues in the design of suspension bridges: the interaction between the stiffening girder and the wind load. After the accident, new studies on the effect of wind loads led to the construction of stiffer girders and modification of existing structures such as the Golden Gate Bridge itself.

3. Case Study: Modelling a Suspension Bridge on Strand7

The notation adopted in this chapter follows the one used in "*Cables Supported Bridges*" (Gimsing 1997), as the formulas reported in the text book are going to be used. There might therefore be some discrepancies from the previous chapter (literature review).

- **Assumption for the Design of the Cable System**

Traffic and concentrated loads are initially neglected in the preliminary design phase as their contribution is negligible compared to the one due to self weight.

This assumption is in accordance with what is reported in various text books such as "*Cables Supported Bridges*" (Gimsing 1997) and "*The Theory of Suspension Bridges*" (Pugsley 1968). The accuracy of this assumption will be investigated in the following paragraphs and finally commented.

3.1. Materials

3.1.1. Girder and Pylons

The pylons and the truss girder will be composed of steel elements having the properties given by the "Structural Steelwork" section in Strand7's library. The relevant values are reported in Table 3.1-1 below:

Table 3.1-1

Girder and Pylons' Properties		
Modulus of Elasticity	E	200 [GPa]
Density	γ	7850 [kg/m^3]

3.1.2. Cables and Hangers

The suspension cables and hangers will be modelled using the "cutoff bar" option in Strand7, assigning a gross circular cross sectional-area to the elements. The materials' properties will be those given by "Structural Steelwork" in Strand7's library. The Modulus of Elasticity (E) and the Design Stress (fcbd) are taken in accordance to "Cables Supported Bridges" (Gimsing 1997), and the relevant values are reported in Table 3.1-2:

Table 3.1-2

Cables and Hangers' Properties		
Modulus of Elasticity	E	200 [GPa]
Design Stress	f_{cbd}	800 [MPa]
Density	γ_{cb}	7850 [kg/m^3]

3.1.3. Concrete Deck

A concrete deck will be considered in order to emulate part of the self-weight of the structure. The main characteristics are reported in table 3.1-3 below:

Table 3.1-3

Concrete Deck		
Membrane Thickness	s_c	0.25 [m]
Concrete Type	Compressive Strength f_c = 32 MPa	
Density	γ_c	2400 [kg/m^3]
Modulus of Elasticity	E_c	30.96 [GPa]

3.2. Defining Span Proportions and Lengths

First of all the total length of the suspension bridge has to be determined. The total length will be given by the length of the main span (L_m) and the two side-spans ($2 \cdot L_a$).

As far as the main span is regarded, a length of 960[m] is chosen for the ongoing analysis, a value that fits with practical experience. For the determination of the side spans' length, reference can be made to "*Cables Supported Bridges*" (Gimsing 1997). Three-span suspension bridges are generally classified as:

- Suspension bridges with short side spans

$$L_a \leq 0.3 \cdot L_m$$

- Suspension bridges with long side spans

$$0.4 \cdot L_m < L_a \leq 0.5 \cdot L_m$$

An initial length ratio of 0.25 is therefore chosen, thus leading to the dimensions reported in Table 3.2 below:

Table 3.2

Spans' Dimensions		
Span Ratio	r_L	0,25
Main Span Length	L_m	960 [m]
Side Span Length	$L_a = 0.25 \cdot L_m$	240 [m]
Total Length	$L_m + 2 \cdot L_a$	1440 [m]

3.3. Truss Girder

The truss girder model is based on the Golden Gate Bridge's girder, designed with the help of the available images and a similar model kindly provided by Professor Peter Ansourian of The University of Sydney. As the main focus of this work is to compare theoretical and software-based results, the elements composing the truss girder were not designed in detail but in order to obtain a reasonable model to be adopted in further analysis. A series of images are shown below depicting the structure of a single unit of the truss girder (Figures 3.1 - 3.2 - 3.3). This unit is thirty (30) meters wide , thirty (30) meters long and seven and a half (7.5) meters in depth. This unit will be copied along the z-axis in order to form the 1440 [m] long girder:

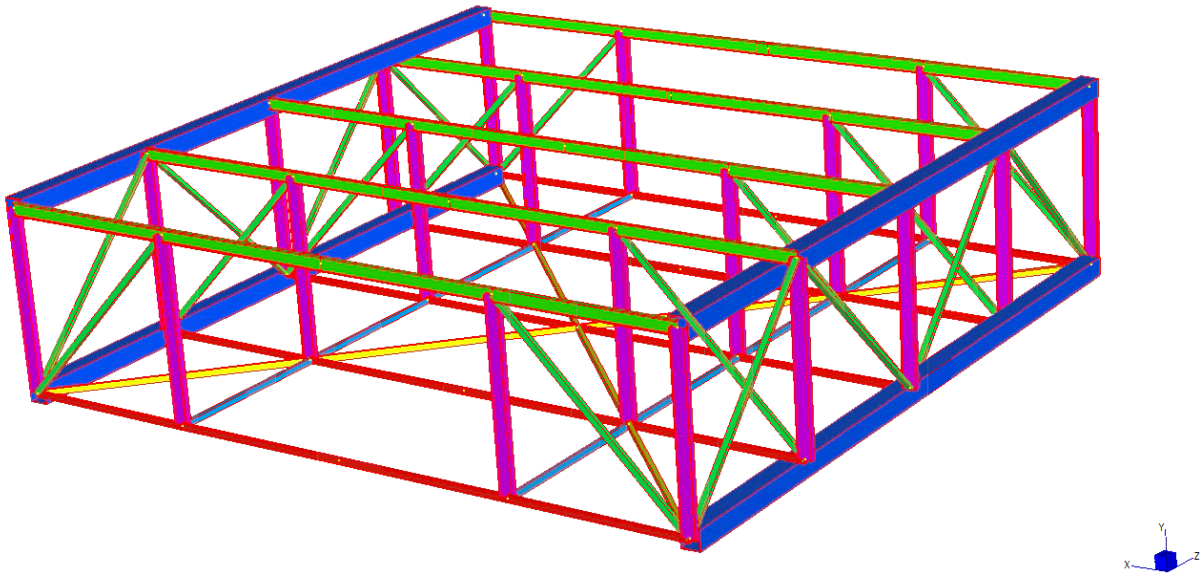

Figure 3.1: Single unit of the truss girder.

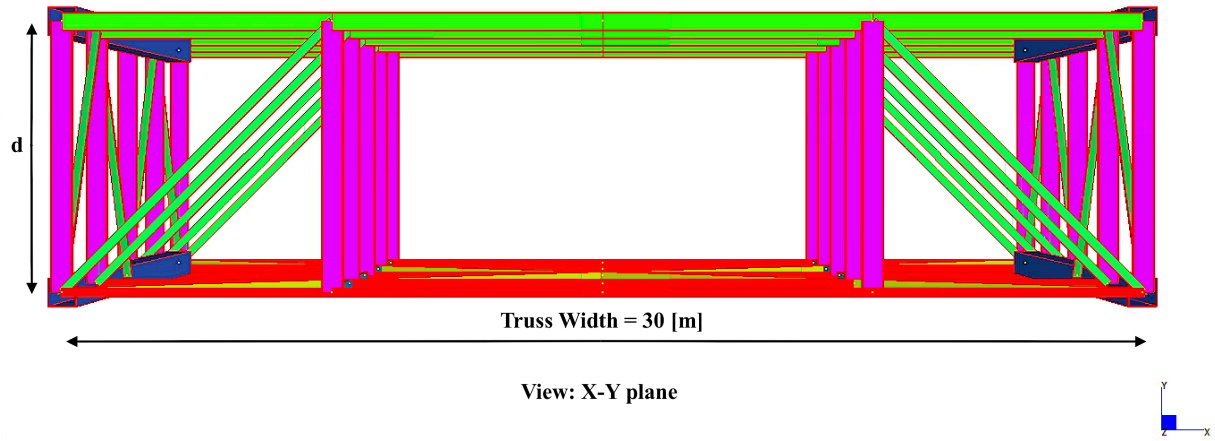

Figure 3.2: Single unit of the truss girder, X-Y plane view.

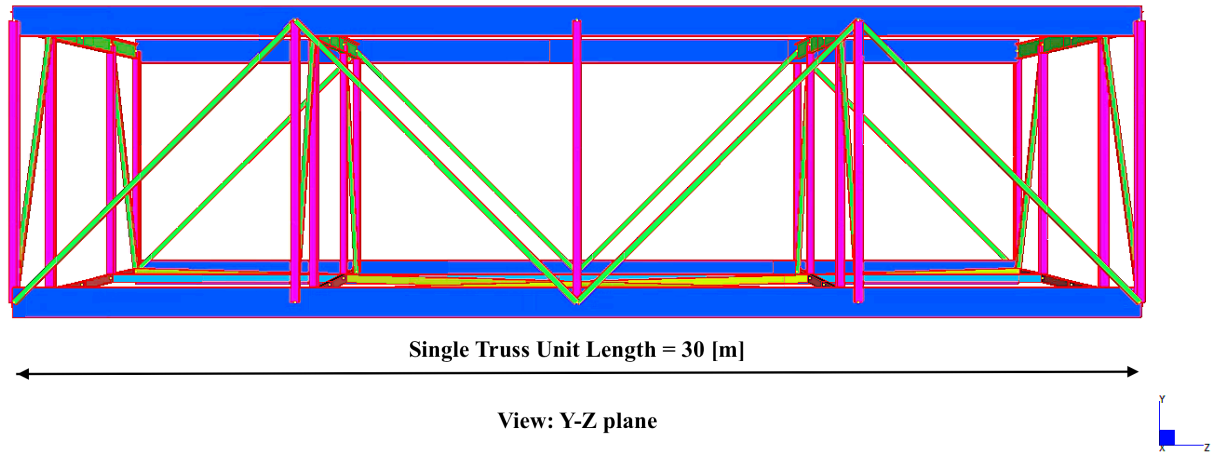

Figure 3.3: Single unit of the truss girder, Y-Z plane view.

The relevant values for the unit just shown are reported in Table 3.3-1 below:

Table 3.3-1

General Girder Dimensions		
Girder Depth	d	7.5 [m]
Truss Width	30 [m]	
Single Truss Unit Length	30 [m]	

The following chart (Table 3.3-2) contains a list and relevant details of the elements adopted for the truss girder model. The Strand7 notation for structural elements' dimensions is also reported in the right bottom side of the chart:

Table 3.3-2

Truss Girder's Elements			
Beam Property 1 (Square Hollow Section) B=D=0.8 [m] T1=T2=0.02 [m] — A=0.0624 [m²] I_{11}=0.00633152 [m⁴]	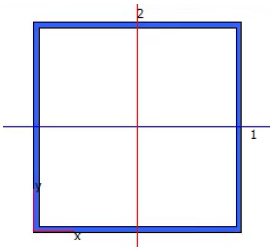	**Beam Property 2** (RHS 250x150x9) B=0.15 [m] D=0.25 [m] T1=T2=0.009 [m]	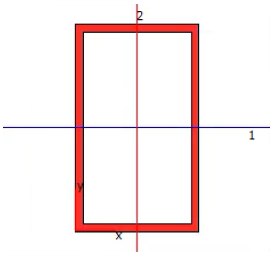
Beam Property 3 (IPE 500) B1=B2=0.20 [m] D=0.50 [m] T1=T2=0.016 [m] T3=0.0102 [m]	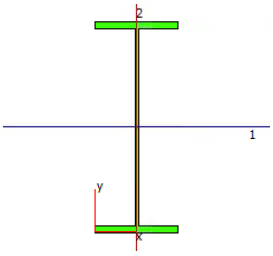	**Beam Property 4** (RHS 250x150x9) B=0.15 [m] D=0.25 [m] T1=T2=0.009 [m]	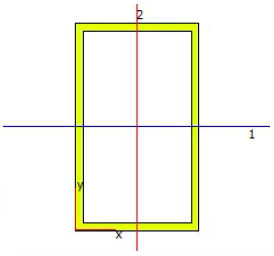
Beam Property 5 (RHS 250x150x9) B=0.15 [m] D=0.25 [m] T1=T2=0.009 [m] A=0.0066 [m²] I_{11}=0.00005370 [m⁴]	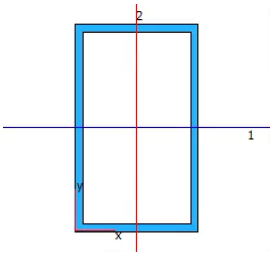	**Beam Property 6** (IPE 600) B1=B2=0.22 [m] D=0.60 [m] T1=T2=0.019 [m] T3=0.012 [m]	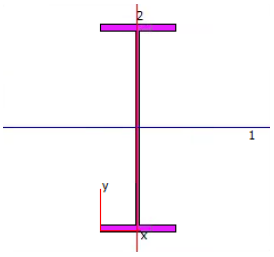
Beam Property 7 (RHS 250x150x9) B=0.15 [m] D=0.25 [m] T1=T2=0.009 [m]	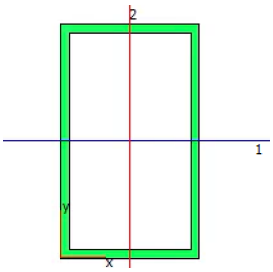	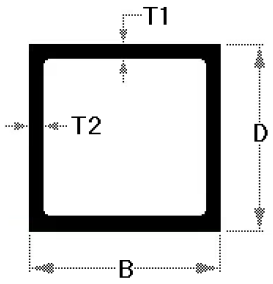	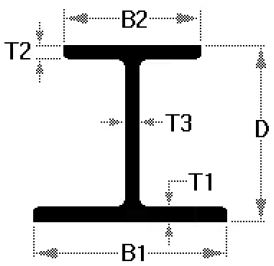

The Uniformly Distributed Load (UDL) due to the girder and concrete deck's self weight to be adopted in future calculations are reported in Table 3.3-3 below:

Table 3.3-3

Dead Load Determination - Self Weight Only		
Continuous Structural Elements Over the Entire Length of the Bridge		
Element Name	UDL [kN/m]	% of Total Load
Beam Property 1	19,22	1,36
Beam Property 4	1,44	0,10
Beam Property 5	1,02	0,07
Beam Property 7	1,44	0,10

Non Continuous Structural Elements		
Element Name	UDL [kN/m]	% of Total Load
Beam Property 2	208	14,72
Beam Property 3	367	25,91
Beam Property 6	493	34,84
Beam Property 7	147	10,41
Concrete Deck		
Element Name	UDL [kN/m]	% of Total Load
Plate Property 1	176,58	12,48
Resulting Total Dead Load (g) g_{tot} = 1415 kN/m		

Note: in the calculation listed in the following paragraphs, half of the UDL has to be considered because there are two planes of cables supporting the bridge. Reference will thus be made to ($g_{tot}/2$):

$$\frac{g_{tot}}{2} = 707.5 \text{ kN/m}$$

3.4. Hangers

A. Central Hanger's Length

The central hanger's length is usually in the range of 3-10[m] (Gimsing 1997). For the purpose of the ongoing investigation a value of 3[m] has been selected.

Once the main cable's sag will be known, the top pylon's coordinate will be given by the summation of the central hanger's length and the sag itself. All the other hangers will be ultimately connected once the cables and the truss girder are modelled. The design value is reported in Table 3.4-1:

Table 3.4-1

Central Hangers' Length	
j_m	3 [m]

B. Hangers' Spacing

In order to properly model the connection between the girder and the suspension cables, the hanger spacing (λ) needs to be predetermined. Once again a value of 15[m] (reported in Table 3.4-2) is chosen following practical examples (the Golden Gate Bridge has the same spacing).

Table 3.4-2

Hangers' Spacing	
λ	15 [m]

C. Hangers' Diameter

The hangers' diameter is determined by following the preliminary design guidelines given in "*Cables Supported Bridges*" (Gimsing 1997). There are two assumption on which this calculation is based:

i. The hangers will carry the distributed load acting on a length of the stiffening girder equal to the hanger spacing (λ).
ii. Concentrated forces (P) are represented by a uniformly distributed load acting on a length equal to thirty times the depth of the girder (30·d).

Given these assumptions and the relative scheme shown in Figure 3.4 below, the maximum hanger force is determined as:

$$T_h = (g+p)\lambda + P\frac{\lambda}{30 \cdot d}$$

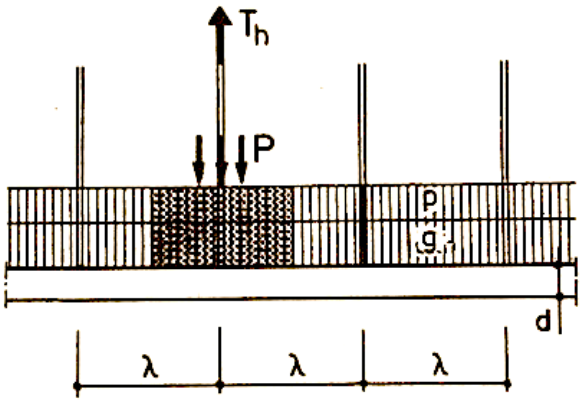

Figure 3.4: Loading case for maximum hanger force (Gimsing 1997).

Considering that:

$$\begin{cases} g = \dfrac{g_{tot}}{2} = 707.5 \text{ kN/m} \\ p = 0 \text{ kN/m} \\ P = 0 \text{ kN} \\ d = 7.5 \text{ m} \\ \lambda = 15 \text{ m} \end{cases} \quad \Rightarrow \quad T_h = 10612 \text{ kN}$$

Note that the traffic and concentrated loads are neglected at this stage because their contribution is negligible compared to that of self weight. Moreover, concentrated forces are assumed to be redistributed along a length equal to thirty times the depth of the girder:

$$P\frac{\lambda}{30 \cdot d} = P\frac{15}{30 \cdot 7.5} = \frac{1}{15}P$$

The cross-sectional area can now be determined as:

$$A_h = \frac{T_h}{f_{cbd}} = \frac{10612 \cdot 10^3}{800} = 0.013 \text{ m}^2$$

Hence the diameter for all the hangers will be (as reported in Table 3.4-3):

$$D_h = \sqrt{\frac{4 \cdot A_h}{\pi}} \simeq 0.130 \text{ m}$$

Table 3.4-3

Hangers' Diameter	
D_h	0.150 [m]

As shown in Figure 3.5 below, the hangers will be connected to the girder with a spacing of λ=15 [m]:

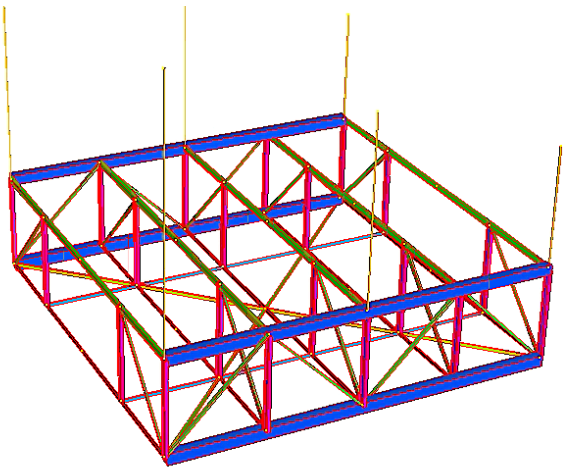

Figure 3.5: Hangers' connection to the truss girder.

3.5. Cables' Profile Definition and Preliminary Design

In order to model the suspension cables on Strand7 it is necessary to first determine the shape to be adopted (catenary or parabola). Strand7 permits the user to model a "cable" element but this would not be composed of the nodes required to connect the suspension cables to the stiffening girder by means hangers. It is therefore required to create the nodes of the suspension cable as points of a parabolic or catenary curve. An investigation of the accuracy of the two shapes is carried out in the following paragraph.

3.5.1. Catenary VS Parabola

In order to decide if the shape to be adopted is the one of the catenary or the parabola, a brief example will be shown below. As already discussed in the literature review, the catenary curve and the parabolic curve diverge at a sag ratio of 0.15 (Walter Podolny 1976). In order to verify the accuracy of this result, two cables having different sag ratios have been modelled using both the catenary and the parabolic equations. The design parameters and relevant dimensions are reported in Table 3.5-1 below.

- **Step 1 - Modelling the cable on Strand7**

Table 3.5-1

Relevant Design Parameters	Cable_1	Cable_2
Diameter (D)	0.934 [m]	0.934 [m]
Horizontal Chord's Length (L)	1260 [m]	1260 [m]
Cable's Free Length (l)	1550 [m]	1307 [m]
Sag (d)	399,0987	152.0939 [m]
Sag Ratio (d/L)	**0,32**	**0,12**
Horizontal Component of Tension (T_0)	29,188,471.69 [N]	70,099,084.39 [N]
Weight of cable/unit length (μ)	52,762.08 [N/m]	52,762.08 [N/m]

The horizontal component of tension in the cable T_0 is due to the cable's self weight only.
The two cables just analysed have no internal nodes to be connected to hangers. The following step is therefore necessary to create these nodes.

- **Step 2 - Creating the Catenary and Parabolic Curved Cable**

Once the horizontal component of the tension (T_0) in the cable is known, its value can be used and substituted in the equation for the catenary provided in paragraph 2.1.1. The sag value

obtained from the catenary equation is then used in the determination of the parabolic shape of the cable (following the formulas in paragraph 2.1.2). This way, given the same sag "d" for the two shapes, an evaluation of the most accurate shape can be carried out:

$$\text{Catenary:} \quad y = c \cdot \cosh\left(\frac{x}{c}\right) = \frac{T_0}{\mu} \cdot \left[\cosh\left(\frac{x\mu}{T_0}\right) - 1\right]$$

$$\text{Parabola:} \quad \begin{cases} y = \frac{1}{2}\frac{\mu}{H} \cdot x^2 \\ H = \frac{\mu L^2}{8 d_c} \end{cases}$$

The sag value "d_c", obtained from the catenary equation, and the horizontal component of tension in the cable "H" for the two analysed cables are reported in Table 3.5-2 below:

Table 3.5-2

Obtained Results	Cable_1	Cable_2
d_c	399.2092 [m]	152.1890 [m]
H	26,228,442.28 [N]	68,800,17.06 [N]

The obtained sets of coordinates are reported in Tables A3.1 and A3.2 in the Appendix and can be copied and pasted on Strand7 in order to create the connection nodes for the sagging cables. These nodes will then be connected with "cutoff bar" elements in order to model the suspension cables for the bridge's model.

- **Step 3 - Verifying the Accuracy of Results**

The obtained profiles are plotted in Figures 3.6 and 3.7 below:

Figure 3.6: Cable_1 - Catenary vs Parabola

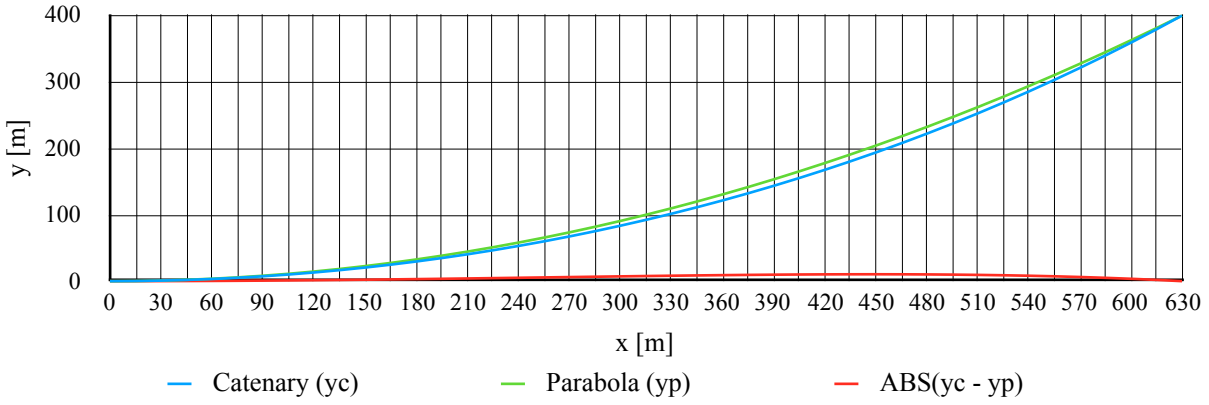

Figure 3.7: Cable_2 - Catenary vs Parabola

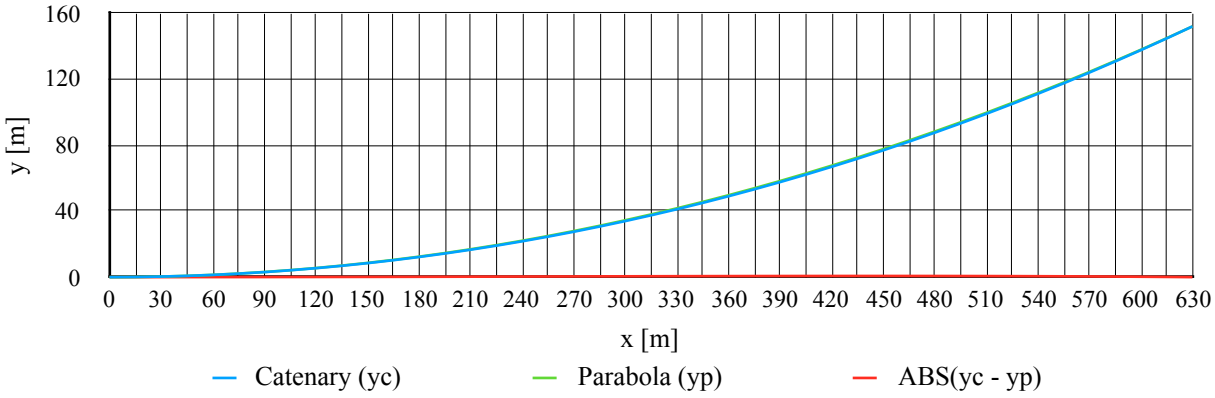

As it can be noticed from the plots shown above the discrepancy between the catenary and the parabolic curve for Cable_1 (having sag ratio equal to 0.32) is greater than the one for Cable_2 (having a sag ratio of 0.12). This agrees with our expectation as the sag ratio for Cable_1 is larger than 0.15. In particular, the maximum discrepancy on the y-axis for the two cables are reported in Table 3.5-3 below:

Table 3.5-3

Maximum discrepancy	**Cable_1**	**Cable_2**
max (y_c - y_p)	10.34 [m]	0.71 [m]
max (y_c - y_p)/d	2,6%	0,46%

Moreover, there is a small discrepancy between the sag given by Strand7 and the catenary equation. This is probably due to the accuracy of the horizontal component of tension in the cable obtained on Strand7 and to be used as an input for the catenary equation. However, this does not represent a problem as the 0.03% - 0.06% error observed does not affect any design factor. These discrepancies are reported in Table 3.5-4 below:

Table 3.5-4

	d (Strand7)	d_C (Catenary Eq.)	Discrepancy
Cable_1	399,0987	399,2092	0,03%
Cable_2	152,0939	152,1809	0,06%

Conclusions:

The parabolic curve represents the shape adopted by the freely hanging cable with a satisfying accuracy for sag ratios smaller than 0.15. For this reason, both the catenary and the parabolic shapes can be adopted for the model of the suspension bridge as its sag ratios are usually in

the range 0.08 - 0.12. It is therefore plausible to rely on the simplified equations based on the parabolic shape that can be often encountered in literature.

The procedure adopted for the creation of the nodes on Strand7 will not be shown again in the ongoing analysis as it is the same as the one just presented.

3.5.2. Main Suspension Cable

A. Sag Ratio and Cable Profile Definition

The first parameter to be determined at this stage is the sag ratio of the main cable. As already reported in the literature review, typical sag ratios for the main span are in the range of 0.08-0.12 (Pugsley 1968; Gimsing 1997). The chosen value for the purpose of this project and the resultant sag are therefore reported in Table 3.5-5 below:

Table 3.5-5

Sag and Sag Ratio - Preliminary Assumption	
k^*_m	96 [m]
$s^*_{r,m}$	0,10

The chosen sag ratio represents a good compromise for material and stiffness optimisation: a larger sag would minimise the use of material whilst a smaller sag would improve stiffness (Gimsing 1997).

The adopted value of the diameter is initially assumed as 0.8[m] (as reported in Table 3.5-6), similarly to the one adopted for the Golden Gate Bridge's suspension cable.

Table 3.5-6

Diameter - Preliminary Assumption		
Diameter	D_1	0.8 [m]
Weight of the Cable / Unit Length	μ_m	38.71 [kN/m]

This initial diameter will be probably refined in the following paragraphs and its value may actually change. However, having a pre-defined geometry eases the initial Strand7 phases of modelling in which it might be interesting to test the single cable itself. In fact, when testing the cable alone, the girder's properties and thus its dead load might not be known.

It can be now modelled the single "cable" element on Strand7 in order to get the value of the horizontal component of tension in the cable (T_0) due to self-weight, to be adopted for the

determination of the catenary's nodes. The procedure has already been explained in the previous paragraph and will not be entirely reported here.

Strand7 will require to insert a "cable free length" value that matches with the designed sag. Instead of guessing this value, reference can be made to formula (10) of paragraph 2.1.2 of the Literature Review in order to have an accurate estimation. In this situation we can notice how parabola-based formulas can be useful. The formula is rewritten here using the Gimsing notation:

$$\mathrm{L}_{m,f} = L_m \cdot \left[1 + \frac{8}{3} \left(\frac{k_m^*}{L_m} \right)^2 \right] = 985.60 \text{ m}$$

The resulting sag given in Strand7 will be slightly different from the one initially assumed (96 m) as reported in Table 3.5-7 below:

Table 3.5-7

Design Sag and Sag ratio - Strand7 Model	
k_m	97.83 [m]
$s_{r,m}$	0,102

However, this discrepancy does not represent an issue as the sag ratio has changed by 2% only. The obtained sag value is to be used in all the following calculations.

The horizontal component of the tension in the cable obtained via Strand7 analysis is reported in Table 3.5-8:

Table 3.5-8

Horizontal Component of Tension in the Cable	
T_0	46200.41 [kN]

Once again it is interesting to compare the Strand7's result for T_0 with the one given in paragraph 2.1.2. (rewritten for Gimsing notation). The horizontal component of tension in the cable given by the parabola-based formula is:

$$T_{0,parabolic\ shape} = \frac{\mu_m \cdot L_m^2}{8 k_m} = 45582.72 \text{ kN}$$

The 1.4% discrepancy is acceptable and once again underlines how useful the simplified parabolic-based analysis can be.

It is now possible to evaluate the pylon top coordinate (reported in Table 3.5-9 below). As the (y)-reference plane is located at the top layer of the truss girder (it coincides with the top elements' axis), this will be situated at:

Table 3.5-9

Pylon Top (y) coordinate		
H_{pt}	$k_m + j_m$	100.83 [m]

This coordinate is also used to evaluate the side span cable shape in the relevant paragraph.

By substituting the proper values in the catenary equation already presented we get the nodes of the sagging cable. The step (Δz) to be adopted has to be equal to the hanger spacing (λ) in order to connect the truss girder to the suspension cable with vertical elements (hangers):

$$y = \frac{T_0}{\mu_m} \cdot \left[\cosh\left(\frac{z\mu_m}{T_0} \right) - 1 \right]$$

The plot showing the nodes and the cable shape (the right half of it) is schematically shown in Figure 3.8 below (not in scale):

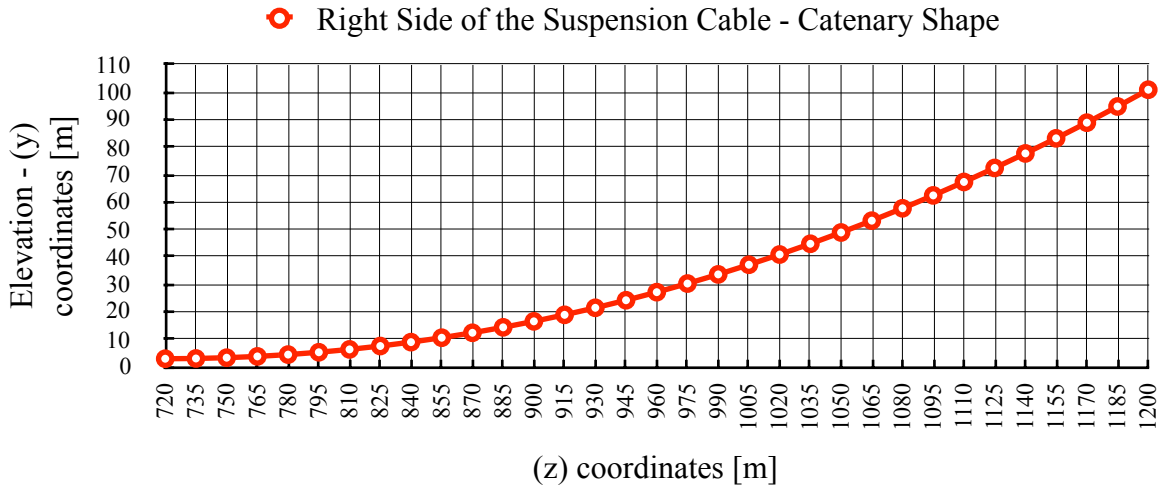

Figure 3.8: Catenary shape for the Strand7 model.

The obtained coordinates are also reported in Table A3.3 in the Appendix.

Note that the bottom left node represented in the plot corresponds to the cable's node at midspan, having the following coordinates:

$$(y\ ,\ z)_{Midspan} = \left(j_m\ ,\ L_a + \frac{L_m}{2}\right) = (3\ ,\ 720)m$$

Whilst the top right node corresponds to the cable's node at the top of the pylon, having the following coordinates:

$$(y\ ,\ z)_{PylonTop} = \left(H_{pt}\ ,\ L_a + L_m\right) = (100.83\ ,\ 1200)m$$

The so obtained cable will be mirrored on Strand7 in order to obtain the entire main cable.

B. <u>Refining the Main Cable's Diameter</u>

Now that the main elements composing the model are defined, it is possible to refine the diameter of the main cable, reference is made to the book "Cable Supported Bridges" (Gimsing 1997). If the following assumptions are adopted:

i. The hangers' dead load can be neglected as its contribution is quite small
ii. Traffic load (p) and concentrated forces (P) are neglected at this stage because they are usually negligible compared to the girder's self weight

Then the area of the cable can be calculated as:

$$A_m = \frac{\left[\left(\frac{g_{tot}}{2} + p\right)L_m + 2P\right]\sqrt{L_m^2 + 16k_m^2}}{8 f_{cbd} k_m - \gamma_{cb} L_m \sqrt{L_m^2 + 16k_m^2}}$$

Where:

$$\begin{cases} g = \dfrac{g_{tot}}{2} = 707.5 \text{ kN/m} \\ p = 0 \text{ kN/m} \\ P = 0 \text{ kN} \\ L_m = 960 \text{ m} \\ k_m = 97.83 \text{ m} \\ \gamma_{cb} = 77 \text{ kN/m}^3 \end{cases} \quad \Rightarrow \quad A_m = 1.281 \text{ m}^2$$

Hence the diameter:

$$D_m = \sqrt{\frac{4 \cdot A_m}{\pi}} = 1.277 \text{ m}$$

The adopted refined value is thus reported in Table 3.5-10:

Table 3.5-10

Diameter - Refined Dimension		
Diameter	D_m	1.2 [m]
Cross-sectional Area	A_m	1.13 [m^2]
Weight of the Cable / Unit Length	μ_m	87.1 [kN/m]

Now that a new value of the diameter has been determined, the freely hanging cable's profile should be adjusted. However, as the difference would be quite small, the shape already adopted will not be changed. Moreover, it must be taken into consideration that changing the cable's shape is time consuming and we might come across other changes for analytical reasons.

3.5.3. Side Suspension Cables

The sag ratio is the first parameter to be determined. A typical rule of thumb reported in text books for the given geometry suggests that this is taken as one fourth (1/4) of the main cable's sag ratio (Pugsley 1968; Gimsing 1997). However, the text book "Cable Supported Bridges" (Gimsing 1997) provides an estimation of the sag ratio based on:

- The magnitude of the distributed loads acting on the girder
- The geometry of the system (span lengths and sags)
- The quantity of cable steel

It is therefore interesting to evaluate the sag ratio according to both methods and determine whether they comply with one another or not.

After the sag is determined and hence the cables' shape, the diameter of the side span cables will be calculated as well.

A. <u>Sag Ratio According to the Rule of Thumb</u>

The sag ratio obtained by applying the rule of thumb is reported in Table 3.5-11 below:

Table 3.5-11

Sag Ratio - Rule of Thumb		
$s_{r,a}$	$0.25 \cdot s_{r,m}$	0,0255

B. <u>Sag Ratio According to "Cable Supported Bridges" (Gimsing 1997)</u>

The methodology proposed by "Cable Supported Bridges" is presented below in order to calculate the sag ratio for the side cables.

First of all the concept of "Theoretical quantity of cable steel" is introduced: for a single cable with length l_{cb} and axial force T_{cb} it is defined as:

$$Q_{c,1} = \frac{\gamma_{cb}}{f_{cbd}} T_{cb} \cdot l_{cb}$$

For a system of *n* cable elements:

$$Q_{cb} = \frac{\gamma_{cb}}{f_{cbd}} \sum_{i=1}^{n} T_{cb,i} \cdot l_{cb,i}$$

Given the configuration presented in Figure 3.9 below:

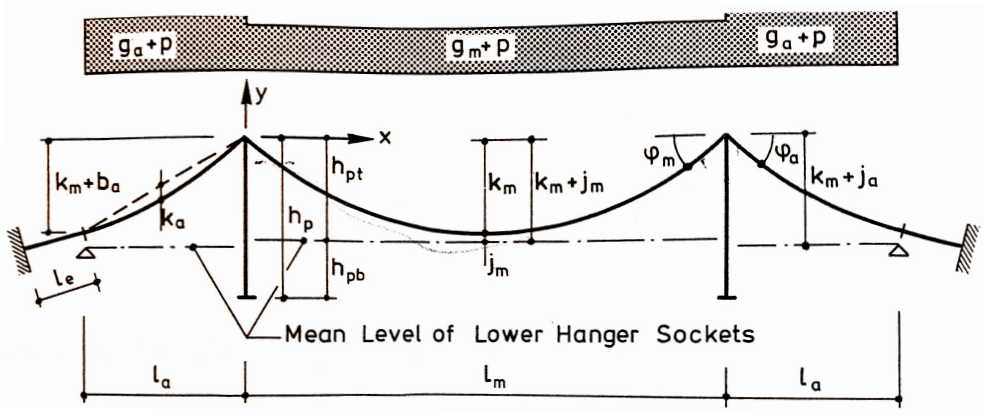

Figure 3.9: Geometrical parameters of a symmetrical suspension bridge (Gimsing 1997).

The sag $k_{a,refined}$ of the side span cable can be calculated as:

$$k_{a,refined} = \frac{\left(g_a + p_a\right) L_a + Q_{ca}}{\left(g_m + p_m\right) L_m + Q_{cm}} \cdot \frac{L_a}{L_m} k_m$$

Where, for our case study:

- $g_a = g_m = g_{tot/2}$
- $p_a = p_m = 0$
- Q_{ca} is the quantity of cable steel in the side span cables
- Q_{cm} is the quantity of cable steel in the main span cable

However, the given formula can be simplified if we consider that the effect of the side span cable's sag on the cable steel quantity is small:

$$k_{a,simplified} = \frac{g_a + p_a}{g_m + p_m}\left(\frac{L_a}{L_m}\right)^2 \cdot k_m$$

Given the particular conditions of our case the result will be:

$$k_{a,simplified} = \left(\frac{L_a}{L_m}\right)^2 \cdot k_m = 6.114 \text{ m}$$

The resulting sag ratio is therefore:

$$s_{r,a} = \frac{k_{a,simplified}}{L_a} = 0.0255$$

As it can be noticed the obtained result matches perfectly with the sag ratio given by the rule of thumb presented before, taken from the text book "The Theory of Suspension Bridges" (Pugsley 1968). It therefore seems reasonable to affirm that the rule of thumb comes from the case just analysed, where the applied distributed load is constant on the three spans, and the side span length is one fourth (1/4) of the main span length, after all these conditions are quite common for cable supported bridges.

After this brief digression, we can resume the estimation of the refined cable's sag. The quantity of cable steel in the main span is:

$$Q_{cm} = \frac{\gamma_{cb}}{f_{cbd}}\left(g_m + p_m\right)L_m^2 \cdot \frac{\sqrt{1+16\left(\frac{k_m}{L_m}\right)^2}}{8\frac{k_m}{L_m} - \frac{\gamma_{cb}}{f_{cbd}}L_m\sqrt{1+16\left(\frac{k_m}{L_m}\right)^2}} \cdot \left[1+\frac{8}{3}\left(\frac{k_m}{L_m}\right)^2\right] = 97357 \text{ kN}$$

Where:

$$\begin{cases} g_m = \frac{g_{tot}}{2} = 707.5 \text{ kN/m} \\ p_m = 0 \text{ kN/m} \\ L_m = 960 \text{ m} \\ k_m = 97.83 \text{ m} \\ \gamma_{cb} = 77 \text{ kN/m}^3 \\ f_{cbd} = 800 \text{ MPa} \end{cases}$$

The quantity of cable steel in the side spans is (the formula accounts for both side cables):

$$Q_{ca} = 2\frac{\gamma_{cb}}{f_{cbd}} H_m \cdot L_a \sqrt{1+\left(\frac{k_m}{L_a}+4\frac{k_{a,simplified}}{L_a}+\frac{b_a}{L_a}\right)^2} \cdot \left[1+\frac{8}{3}\left(\frac{k_{a,simplified}}{L_a}\right)^2+\frac{1}{2}\left(\frac{k_m+b_a}{L_a}\right)^2+\frac{l_e}{L_a}\right]$$

Where:

$$\begin{cases} l_e = 0 \\ b_a = 0 \end{cases}$$

The term "H_m" is the horizontal force exerted by the main suspension cable. This force is calculated assuming a uniform distribution of the cable dead load:

$$H_m = \frac{\left(g_m + p_m\right)L_m^2 + Q_{cm}L_m}{8k_m} = 952527.12 \text{ kN}$$

Thus:

$$\begin{cases} Q_{ca} = 53584 \text{ kN} & \text{(for two side cables)} \\ Q_{ca,1} = 26792 \text{ kN} & \text{(one side cable only)} \end{cases}$$

The refined value of the sag can now be obtained as all the required parameters have been calculated:

$$k_{a,refined} = \frac{\left(g_a + p_a\right)L_a + Q_{ca}}{\left(g_m + p_m\right)L_m + Q_{cm}} \cdot \frac{L_a}{L_m} k_m = 7.04 \text{ m}$$

The refined sag ratio to be used on Strand7 is thus reported in Table 3.5-12 below:

Table 3.5-12

Sag and Sag Ratio - Refined Value	
$k_{a,refined}$	7.04 [m]
$s_{r,a,refined}$	0,0293

From the obtained result we can see how the rule of thumb provides a useful and quick method to evaluate the side span's sag ratio. It is therefore reasonable to make use of it for preliminary design purposes.

C. Side Cables' Shape Definition

In order to determine the shape of the cable it is very useful to refer to "Construction and Design of Cable-Stayed Bridges" (Walter Podolny 1976). The required information are reported in the literature review, in particular we may refer to the section "Cable with Inclined

Chord" where the distance (y_D) of the sagging cables' points from the inclined chord is expressed as:

$$y_D = \frac{4f'}{L^2}\left(Lx - x^2\right)$$

As we need to comply with the Strand7 model and design guidelines adopted, the equation is rewritten according to the notation used in chapter 3:

$$y_D = \frac{4k_{a,refined}}{L_a^2}\left(L_a z - z^2\right)$$

This equation is plotted in the graph below (Figure 3.10). As previously mentioned, the step Δz has to be equal to the hanger spacing (Δz=15m). Moreover, as the plot refers to the side cable on the right side of the bridge, its origin on the z axis will be at $z = L_a+L_m$ (z=1200m):

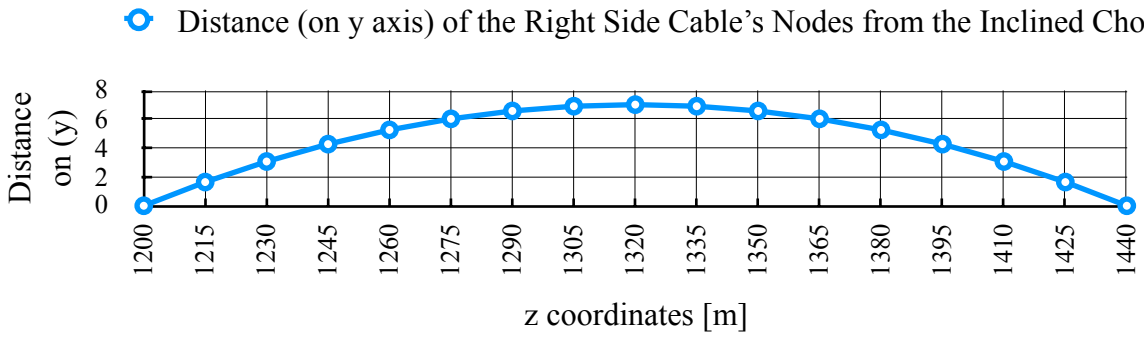

Figure 3.10: Distance of the cable's nodes from the inclined chord.

Moreover, the equation of the inclined chord is expressed as (for the right side span):

$$y_C = H_{pt} - \frac{H_{pt}}{L_a} z$$

By adopting the same step Δz previously used we get the following plot (Figure 3.11):

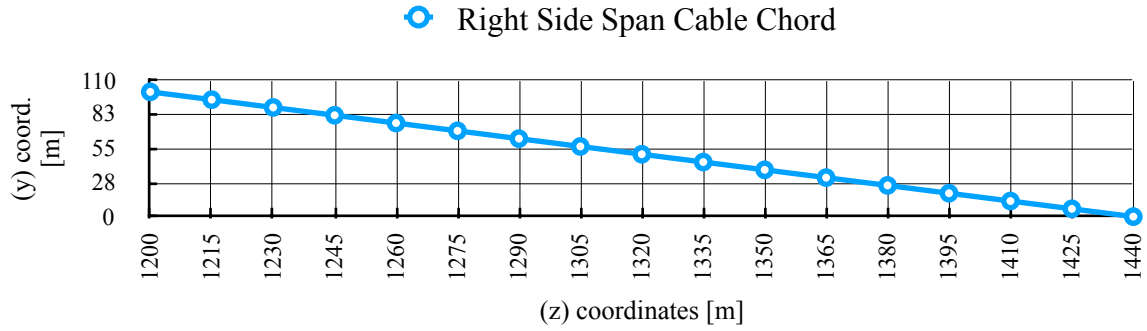

Figure 3.11: Inclined chord.

The right side span cable shape can now be determined by combining the two plots together. The plot showing the nodes and the cable shape is schematically shown in Figure 3.12 below (not in scale):

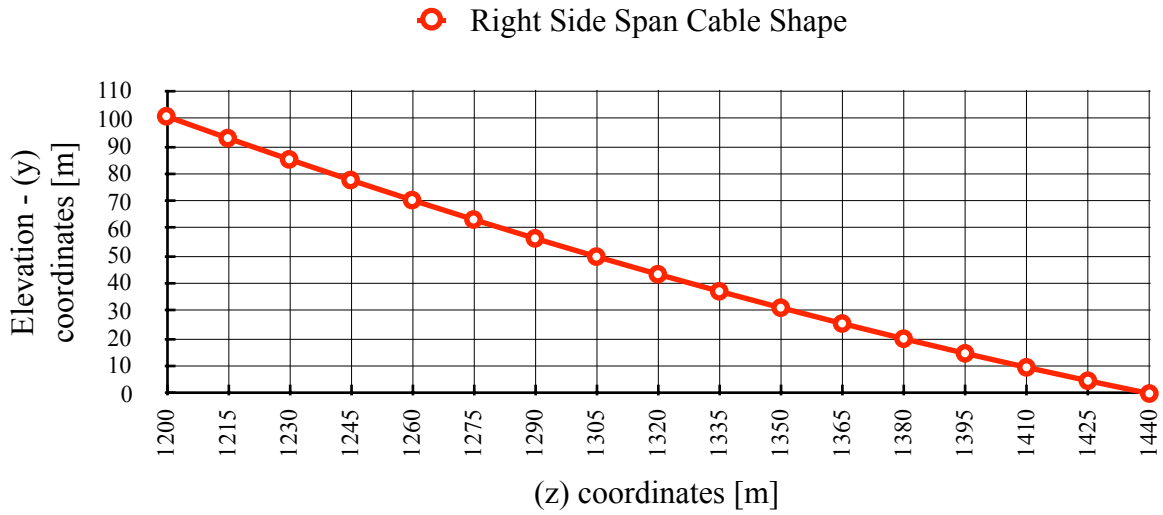

Figure 3.12: Right side span cable shape.

The coordinates of the right side span cable are reported in Table A3.4 in the Appendix.

The overall shape of the cable system is shown below in Figure 3.13 (not in scale):

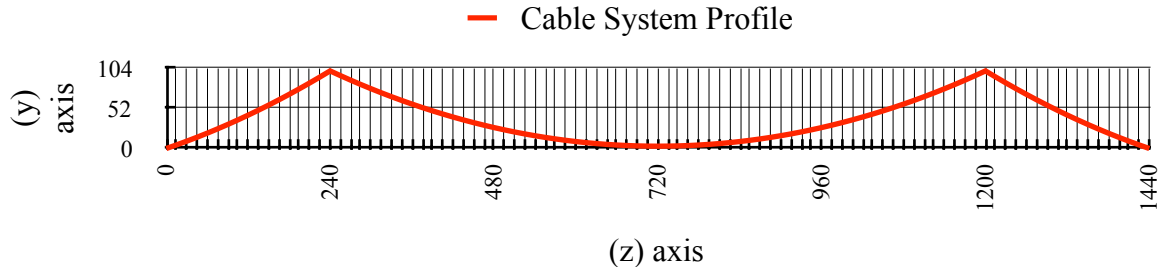

Figure 3.13: Complete cable system (not in scale).

D. <u>Defining the Side Cables' Diameter</u>

The quantity of cable steel calculated for the side span cable can be usefully adopted for the determination of its diameter. Given the obtained quantity (for one side cable only):

$$Q_{ca,1} = 26792 \text{ kN}$$

and the material's density:

$$\gamma_{cb} = 77 \text{ kN/m}^3$$

the volume of required steel is obtained:

$$V_{ca} = \frac{Q_{ca,1}}{\gamma_{cb}} \simeq 348 \text{ m}^3$$

In order to calculate the corresponding area of the cable section, its "cable free length" has to be determined first. Reference can be made to the paragraph "Cable with Inclined Chord" in the literature review where the interested parameter has been reported as (Walter Podolny 1976):

$$S \simeq L \sec \vartheta \cdot \left(1 + \frac{8n^2}{3\sec^4 \vartheta} \right)$$

This is once again rewritten according to the notation used in this chapter:

$$L_{a,f} \simeq L_a \sec \vartheta \cdot \left(1 + \frac{8 \cdot \left(s_{r,a,refined} \right)^2}{3\sec^4 \vartheta} \right)$$

The angle θ is shown in figure 3 of the Appendix and equal to:

$$\theta = \arctan\left(\frac{H_{pt}}{L_a} \right) = 22.79 \text{ deg}$$

Thus the side cable's free length is:

$$L_{a,f} \simeq 260.75 \text{ m}$$

The cross-sectional area of the cable can be finally determined:

$$A_a = \frac{V_{ca}}{L_{a,f}} \simeq 1.33 \text{ m}^2$$

Hence the diameter:

$$D_a = \sqrt{\frac{4 \cdot A_a}{\pi}} \simeq 1.3 \text{ m}$$

For sake of simplicity the side cable's diameter is taken equal to the main cable's one. This way it will also be possible to apply the Steinman's Modified Elastic Treatment further on in the analysis. The relevant design values are reported in Table 3.5-13 below:

Table 3.5-13

Side Cables' Diameter		
Diameter	D_a	1.2 [m]
Cross-sectional Area	A_a	1.13 [m^2]
Weight of the Cable / Unit Length	μ_a	87.1 [kN/m]

Once all the parameters for the design of the cable system are known, the Strand7 model can be implemented. Figures 3.14 below shows an in-scale image of the cable system (pylons are included):

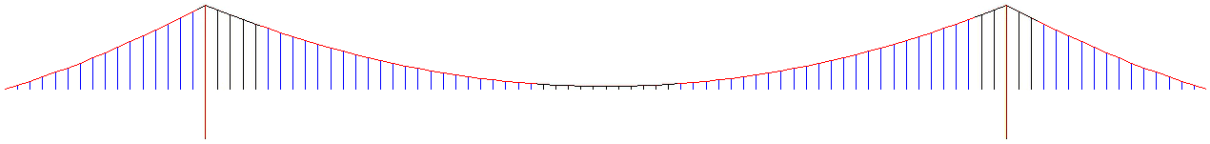

Figure 3.14: Cable system (pylons included).

3.6. Pylons

As already mentioned in the previous paragraph, the pylon top coordinate (y-axis in Strand7) is given by:

$$H_{pt} = k_m + j_m = 100.83 \text{ m}$$

The pylon base coordinate is taken at:

$$h_{pb} = -\ 60 \text{ m}$$

The pylon total height will therefore be:

$$H_{p,tot} = H_{pt} + h_{pb} = 160.83 \text{ m}$$

As the main purpose of this work is to understand the behaviour of the suspension bridge in relation to the cable system, the pylon structure has been defined in order to avoid excessive displacements at the pylon top. The pylon cross-section geometry is reported in Table 3.6:

Table 3.6

Pylon's Geometry		
Beam Property 8 (Solid Rectangular Section) B=16 [m] (along Z on Strand7) D=10 [m] (along X on Strand7)	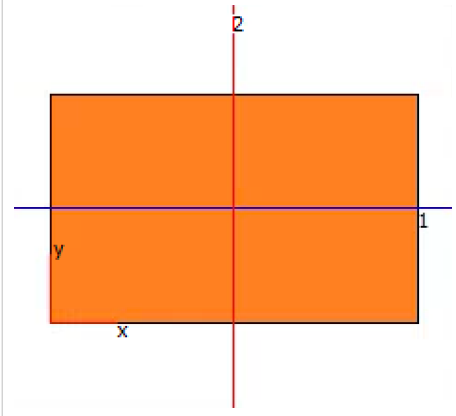	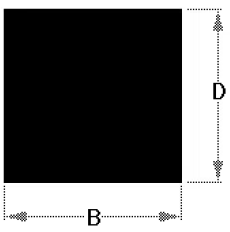

3.7. Strand7 Simulation

Now that every required element for the suspension bridge model has been identified, and its properties determined, a Nonlinear Static analysis can be implemented. Figures 3.15 and 3.16 below show the final state of the designed model:

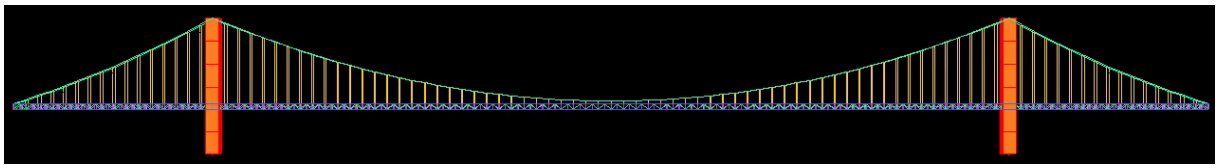

Figure 3.15: Strand7 model, YZ view.

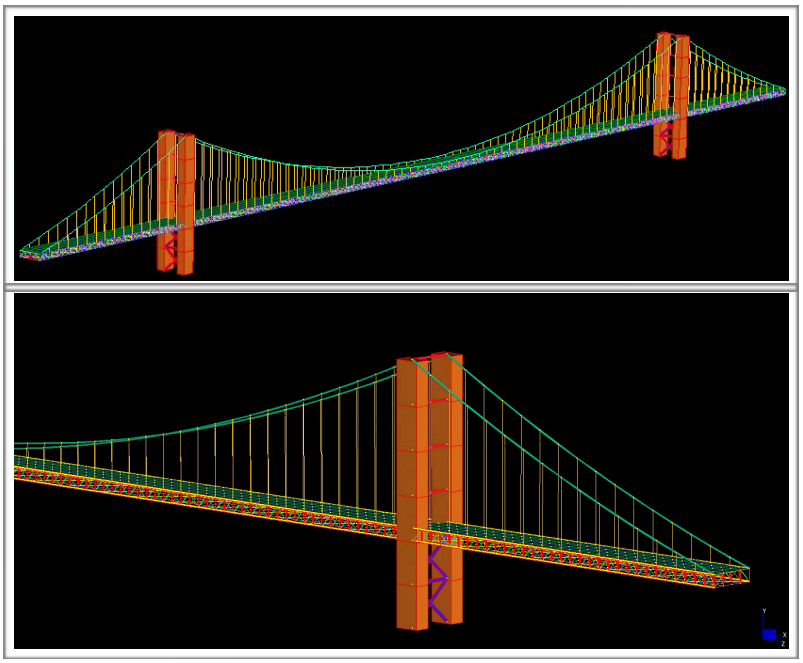

Figure 3.16: Strand7 model, other views.

Prior to conducting any type of analysis, support conditions need to be defined. Once these have been set the linear static analysis can be implemented. Even though the analysis of interest is nonlinear, a brief check of relevant results such as deflection, pylon top displacement and tension in the cables is carried out. The results obtained in the linear analysis will be then compared with those obtained in the nonlinear analysis.

At this stage only dead load will be considered: “Load Case 1: (G)”.

3.7.1. Support Conditions

The support conditions adopted in Strand7 are (refer to Figure 3.17 below for clarity):

- The truss girder is simply supported at four points: the two outer ends (A) and the pylons (B);
- The pylons are fully fixed at their base (C)

- The main and side span suspension cables are continuous over the pylon top (D). They actually form a unique cable element. The so constituted cable system is anchored at the outer girder's ends of the side spans (A, at the deck level) and effectively unrestrained horizontally at the pylons' top (D) by means of the towers' flexibility.

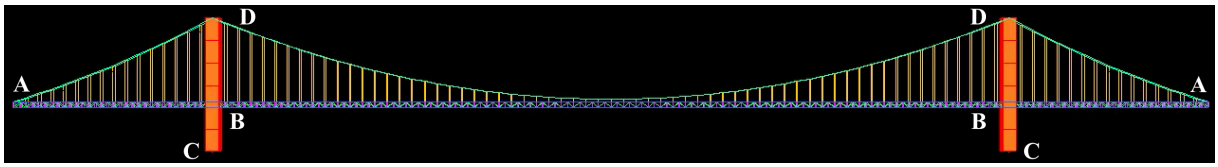

Figure 3.17: Support conditions.

In order to comply with the support schemes generally presented in literature the supports are not developed along the girder's longitudinal axis (z-axis). The simply supported zones in the Strand7 model are therefore lines of points along the transversal axis of the girder (x-axis).

3.7.2. Linear Static Analysis

When performing the Linear static analysis Strand7 will give a warning:

"Warning[123]: Nonlinear behaviour of cutoff bars is ignored by this solver. Use nonlinear solver with material nonlinearity enabled."

However, the nonlinear analysis will be discussed in the following chapter.

The deflected shape due to dead load only is shown in Figures 3.18 and 3.19 below for different scale values:

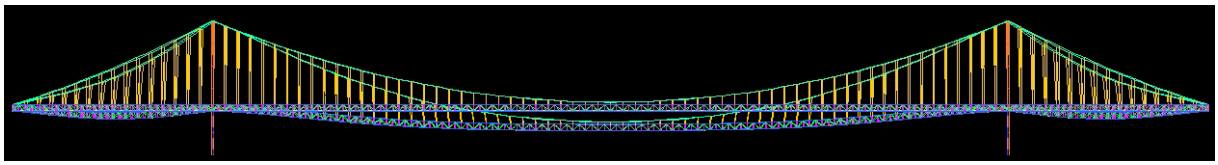

Figure 3.18: Deflected shape, Load Case 1(G). Scale type: absolute, value: 10.

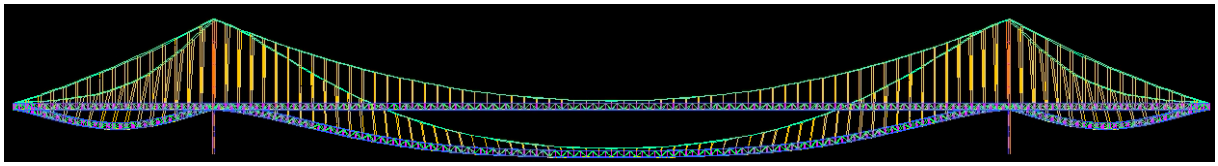

Figure 3.19: Deflected shape, Load Case 1(G). Scale type: percent, value: 5%.

In Tables 3.7-1 and 3.7-2 below some of the relevant results obtained in the linear analysis have been reported.

Table 3.7-1

Linear Static Analysis - Relevant Results for Nodes Displacements		
Result	**Node nº**	**Dimension**
Midspan Deflection δ_m	N. 214	- 2.37 [m]
Side Span Deflection δ_a	N. 194	- 0.96 [m]
Pylons' Top Displacement	N. 1932	Inward: 0.11 [m]

The sign (-) is adopted to indicate downward deflections along the y-axis.

The correspondent deflection to span ratios will thus be:

$$\begin{cases} \dfrac{\delta_m}{L_m} = \dfrac{2.37}{960} \simeq \dfrac{1}{405} & \text{(main spam)} \\ \dfrac{\delta_a}{L_a} = \dfrac{0.96}{240} \simeq \dfrac{1}{250} & \text{(side spans)} \end{cases}$$

Table 3.7-2

Linear Static Analysis - Horizontal Component of Tension in the Cable		
Element Description	**Beam nº**	**Dimension**
Cable element at midspan	B. 4712	228,921.6 [kN]
Cable element at the pylon	B. 4681	228,921.6 [kN]
Side span central element	B. 4673	175,336.8 [kN]
Side span cable element at the pylon	B. 4869	175,336.8 [kN]

As noticeable from the obtained results, the horizontal component of tension in the cable is constant along the cable's length. This result corresponds to what we might expect according to the literature review. However, the linear analysis does not account for the non-linear behaviour of cutoff bar elements and this result may therefore change.

3.7.3. Non-Linear Static Analysis

In order to account for the nonlinear behaviour of cutoff bars, the property adopted for suspension cables and hangers, the cutoff limits have to be set in the beam property window on Strand7. As it is of primary interest to investigate the similarities and/or discrepancies between software and theoretical based results, these limits will be set in order to avoid

restrictive design criteria. As the suspension cables and hangers are meant to be working in tension only, the adopted cutoff limits will be (see Table 3.7-3 below):

Table 3.7-3

Cutoff Limits for Suspension Cables and Hangers	
Max Tension	$1.0x10^{20}$ [N]
Max Compression	$1.0x10^{-3}$ [N]

As per the linear analysis, a series of interesting results is reported in Table 3.7-4 below, referring to Load Case 1 (G) where dead load only is considered:

Table 3.7-4

Nonlinear Static Analysis - Relevant Results for Nodes Displacements		
Result	**Node n°**	**Dimension**
Midspan Deflection δ_m	N. 214	- 2.37 [m]
Side Span Deflection δ_a	N. 194	- 0.71 [m]
Pylons' Top Displacement	N. 1932	Inward: 0.12 [m]

The correspondent deflection-to-span ratios will thus be:

$$\begin{cases} \dfrac{\delta_m}{L_m} = \dfrac{2.37}{960} \simeq \dfrac{1}{405} & \text{(main spam)} \\ \dfrac{\delta_a}{L_a} = \dfrac{0.71}{240} \simeq \dfrac{1}{338} & \text{(side spans)} \end{cases}$$

An in-scale image of the deflected shape is shown in Figure.3.20 below (deflection is barely perceptible at this scale:

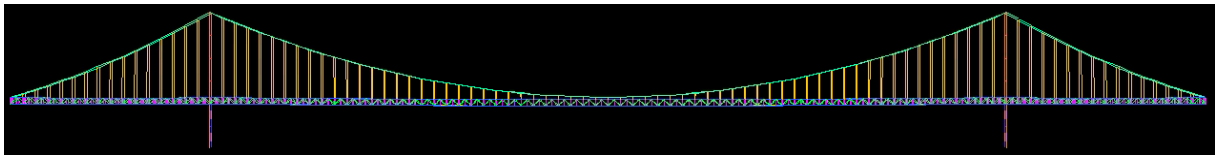

Figure 3.20: Deflected shape, Load Case 1(G). Scale type: absolute, value: 1.

The deformed shape is also reported for different scale values in order to show its trend in Figures 3.21 and 3.22:

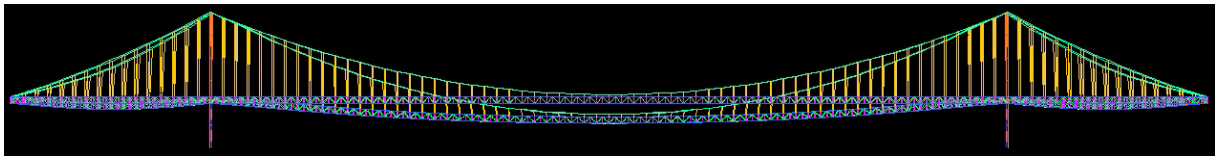

Figure 3.21: Deflected shape, Load Case 1(G). Scale type: absolute, value: 10.

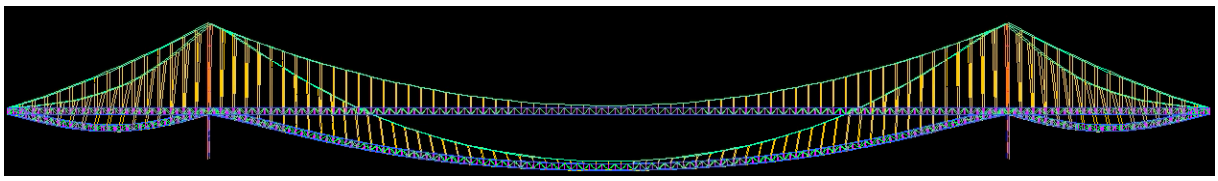

Figure 3.22: Deflected shape, Load Case 1(G). Scale type: percent, value: 5%.

The horizontal component of tension in the cable is reported in Table 3.7-5 below:

Table 3.7-5

Nonlinear Static Analysis - Horizontal Component of Tension in the Cable		
Element Description	**Beam nº**	**Dimension**
Cable element at midspan	B. 4712	222,892.3 [kN]
Cable element at the pylon	B. 4681	223,186.6 [kN]
Side span central element	B. 4673	163,827.1 [kN]
Side span cable element at the pylon	B. 4869	163,863.3 [kN]

The correspondent axial stress in the cable elements are thus reported in Table 3.7-6 below:

Table 3.7-6

Nonlinear Static Analysis - Axial Stress in the Cable		
Element Description	**Beam nº**	**Dimension**
Cable element at midspan	B. 4712	197.08 [MPa]
Cable element at the pylon	B. 4681	212.98 [MPa]
Side span central element	B. 4673	157.55 [MPa]
Side span cable element at the pylon	B. 4869	164.61 [MPa]

The obtained stresses are approximately one fourth to one fifth (1/4 - 1/5) of the design stress f_{cbd} that has been considered in the preliminary design phase:

$$f_{cbd} = 800 \text{ MPa}$$

In contrast to what we have noticed in the linear analysis, the nonlinear analysis gives a non constant value of the horizontal component of tension in the cables. There is a 0.13% variation in the main span cable and a 0.02% variation in the side span cables.

It therefore seems legitimate to inquire if this variation is caused by the change of the cables' sagging shape. However, as this variation is negligible, from now on reference will be made to the horizontal component of tension in the cable as the one measured at the central zones of the cables (beam element 4712 for the main cable and 4673 for the side cables).

3.8. Comparing Steinman's Solution with Software-Based Results

As already reported in the literature review, the development of the Deflection Theory brought to the implementation of numerical approaches to be adopted in the analysis of suspension bridges. These approaches, however, might be arduous and time consuming for preliminary design purposes. Bridge engineers have therefore tried to define approximate methods of analysis so that:

- These methods could be easily applied to the preliminary design phase
- The results they produce are reasonable and of use for design purposes.

It is therefore interesting to analyse one of these methods and to apply it to our case study: the Steinman's Modified Elastic Treatment.

Moreover, the effect of additional applied loads (Live Loads) will also provide proof of the accuracy of the assumption initially adopted for the design of the cable system.

3.8.1. Steinman's Modified Elastic Treatment

As its name suggests, this method reviews the Elastic Theory already presented in the literature review for the case of a symmetrical three-span suspension bridge as the one shown in Figure 3.23 below:

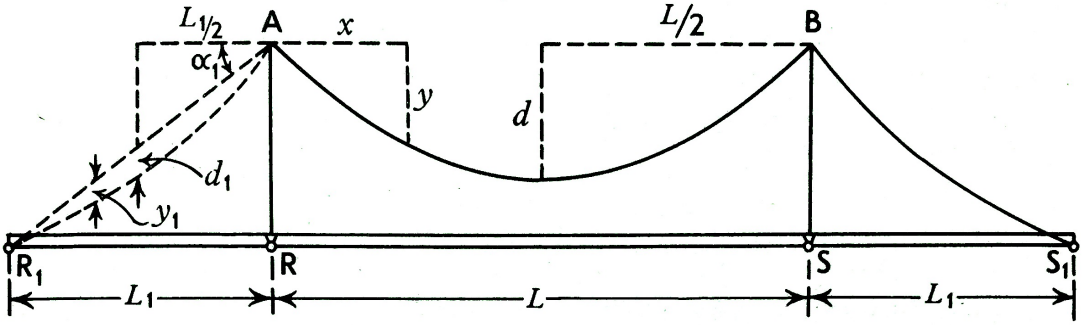

Figure 3.23: Symmetrical three-span suspension bridge scheme (Pugsley 1968).

The assumptions on which Steinman's solution is based are (Pugsley 1968):

- The scheme shown in Figure 3.23 represents the initial form of the bridge subject to its dead load, prior to the application of any live load
- The initial tension in the cable (the set of three cables) due to dead load only will have horizontal component H
- The initial horizontal component of tension in the cable H is constant along the entire length of the bridge (R_1-S_1)

- The cable has the same cross-sectional area A_c and Young modulus E_c along its entire length
- The pylon top (A and B) is free to move horizontally
- There is no bending action in the stiffening girder at this stage (dead load only)
- The effective second moment of area of the main span I is the same for main and side spans.

Based on these assumptions, Steinman has investigated the effect of live loads applied to the stiffening girder on the variation "Δh" of the horizontal component of tension in the cable.
This variation is obtained via Strain Energy Method and has already been reported in the literature review for a single-span suspension bridge:

$$(1) \quad \Delta h = \frac{\frac{Px_1 d}{3EI}\left[L - \frac{x_1^2}{L^2}\left(2L - x_1\right)\right]}{\frac{8Ld^2}{15EI} + \frac{cL}{AE}}$$

The terms in the denominator of formula (3) are referred to the two main contributing elements:

I. Stiffening Girder, contributing for 95%
II. Suspension Cable, contributing for 4-5%

The contribution of suspension rods and pylons is neglected as they account for a fraction of 1% only (Pugsley 1968).
The above relation is thus rewritten for a three-span suspension bridge (Pugsley 1968):

$$(2) \quad \Delta h = \frac{\frac{Px_1 d}{3EI}\left[L - \frac{x_1^2}{L^2}\left(2L - x_1\right)\right]}{\frac{8Ld^2}{15EI} + \frac{16L_1 d_1^2}{15EI_1} + \frac{cL}{AE} + \frac{2c_1 L_1}{A_c E_c}}$$

The two new terms at the denominator (the second and fourth in order) refer to the portion of girder and cable in the side spans. The coefficients "c" and "c_1" are non-dimensional parameters referring to the cable, defined as (Pugsley 1968):

$$(3) \quad \begin{cases} c = 1 + 8\left(\frac{d}{L}\right)^2 \\ c_1 = \left[1 + 8\left(\frac{d_1}{L_1}\right)^2\right] \cdot \left(\frac{1}{\cos\alpha_1}\right)^3 \end{cases}$$

As the numerator of the given formula for Δh refers to the load case in which a concentrated force P is applied in the main span, a general equation can be rewritten for a general loading system:

$$(4)\quad \Delta h = \frac{\frac{1}{E}\left\{\int_0^L \frac{\mu y\, dx}{I} + \int_0^{L_1} \frac{\mu_1' y_1\, dx}{I_1} + \int_0^{L_1} \frac{\mu_1'' y_1\, dx}{I_1}\right\}}{\frac{8Ld^2}{15EI} + \frac{16L_1 d_1^2}{15EI_1} + \frac{cL}{AE} + \frac{2c_1 L_1}{A_c E_c}}$$

The terms μ, μ'_1 and μ''_1 refer to the bending moments in the three spans as if the cable system was absent and the girders simply supported at R_1, R, S and S_1.

Steinman has simplified the calculation of Δh for a series of load cases that might be useful in practical circumstances by means of the so called "Steinman's functions for the application of Elastic Theory". These functions are reported below:

$$(5)\quad \begin{cases} B(k) = k\left(1-2k^2+k^3\right) \\ C(k) = k+k^2-k^3 \\ D(k) = \left(2-k-4k^2+3k^2\right)\cdot(1-k)^2 \qquad \text{for } k = \frac{x}{L} \\ F(k) = \frac{5}{2}k^2 - \frac{5}{2}k^4 + k^5 \\ G(k) = \frac{2}{5}(1-k)^3 - (1-k)^2 + 1 \end{cases}$$

Where "x" is the distance from one of the two ends R1 or R (Figure 3.23 above) to the point of application of the load. The Steinman's functions are plotted in Figure 3.24 below:

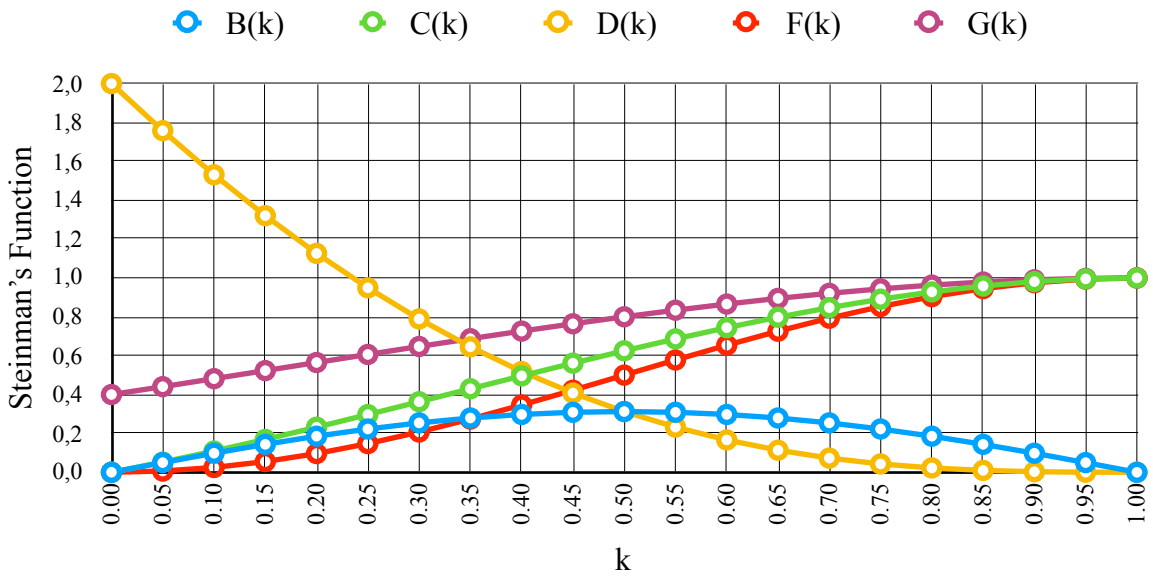

Figure 3.24: Steinman's function plotted for Δk=0.05.

The functions of interest for the evaluation of Δh are B(k) and F(k), whilst the other functions might come of use for bending moment and shear determination in the stiffening girder.

The plotted values of the Steinman's functions are also reported in Table A3.5 in the Appendix.

Two interesting loading cases will now be analysed in order to be compared to Strand7 software's results, in particular:

A. Single load (P) applied on the main span at a distance kL from the pylon (point R)
B. Uniform loading (p) per unit length acting on the main span from the pylon (point R) to a distance kL therefrom

In order to proceed with calculations, an estimate of the second moment of area for the truss girder is required. This is calculated by considering only the contributions of the elements which are continuous along the entire length of the girder (z-axis on Strand7), in particular:

- Beam Property 1
- Beam Property 5

The girder cross section to be analysed is reported in Figure 3.25 below:

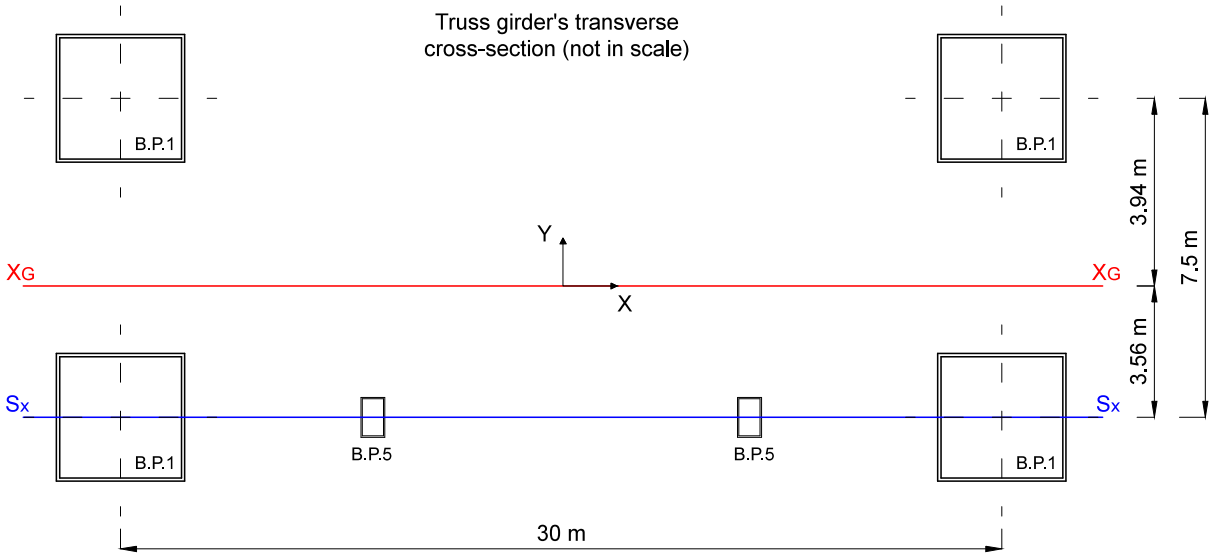

Figure 3.25: Truss girder's transverse cross section (x-y plane).

The obtained second moment of area is reported in Table 3.8-1 below:

Table 3.8-1

Second Moment of Area - Main and Side Spans		
First Moment of Area	S_x	0.936 [m^3]
Second Moment of Area	$I_m = I_a$	3.712 [m^4]

The parameters to be used in the following calculations are reported below, referring to the notation adopted in the preliminary design phase:

$$\begin{cases} L = L_m = 960 \text{ m} \\ L_1 = L_a = 240 \text{ m} \\ d = k_m = 97.83 \text{ m} \\ d_1 = k_{a,refined} = 7.04 \text{ m} \\ A_c = A_m = A_a = 1.13 \text{ m}^2 \\ E = E_c = 200 \text{ GPa} \\ c = 1.083 \\ c_1 = 1.118 \end{cases}$$

A. <u>Single load (P) Applied on the Main Span at a Distance kL from the Pylon (point R)</u>

The variation "Δh" of the horizontal component of tension in the cable is given by the following formula (Pugsley 1968):

$$\Delta h = \frac{L}{Nd} \cdot B(k) \cdot P$$

The term "N" is the denominator of formula (2) reported in this paragraph, multiplied by 3EI/ Ld^2:

$$N = \left(\frac{8Ld^2}{15EI} + \frac{16L_1 d_1^2}{15EI_1} + \frac{cL}{AE} + \frac{2c_1 L_1}{A_c E_c} \right) \cdot \frac{3EI}{Ld^2}$$

$$N = \left[\left(6.6 \times 10^{-3}\right) + \left(0.0171 \times 10^{-3}\right) + \left(0.0046 \times 10^{-3}\right) + \left(0.0024 \times 10^{-3}\right) \right] \cdot \frac{3EI}{Ld^2}$$

$$N = 1.606$$

As noticeable from the reported results, the contribution of the main span girder's portion plays a primary role in the determination of the parameter "N".

The point load (P) to be applied is reported in Table 3.8-2 below:

Table 3.8-2

Point Load	
P	10,000 [kN]

The considered Live Load's magnitude is rather high for a point load as a heavy-weight truck would weight 110 tons approximately (one tenth of the adopted magnitude). However, as the primary aim is to evaluate the accuracy of Steinman's solution, the high-magnitude value

considered will be appropriate. Moreover, this will demonstrate that the effect of Live Loads is negligible during predesign.

The variation "Δh" of the horizontal component of tension in the cable can be now evaluated according to Steinman's function B(k). The results obtained for point loads (P) singularly applied on the main span at a distance kL from the pylon are reported in Table A3.6 in the Appendix and plotted in Figure 3.26 below:

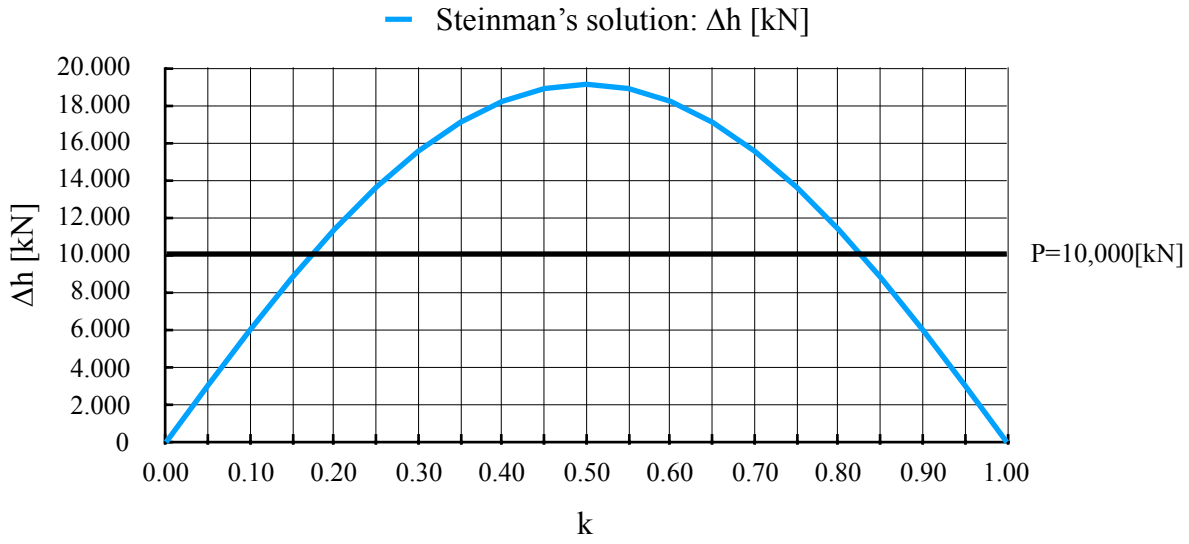

Figure 3.26: Steinman's solution, Δh due to point load (P=10,000 kN).

The maximum variation Δh is found for a point load (P) applied at midspan (k=0.5), its value and the correspondent variation of axial stress in the cable's central element are reported in Table 3.8-3 below:

Table 3.8-3

Maximum Δh	19,097 [kN]
Δσ	16.89 [MPa]

The obtained result shows that the huge concentrated load considered leads to an increase in the horizontal component of tension in the cable of 8.6% only:

$$\frac{19{,}097\ \text{kN}}{222{,}892.3\ \text{kN}} = 0.086 \quad \Rightarrow \quad 8.6\%$$

It is therefore demonstrated that the effect of concentrated loads is negligible in preliminary design.

B. <u>Uniformly Distributed Load (p) Applied from the Pylon (point R) to a Distance kL therefrom</u>

The variation "Δh" of the horizontal component of tension in the cable due to a uniformly distributed load is given by the following formula (Pugsley 1968):

$$\Delta h = \frac{L}{5Nd} \cdot F(k) \cdot pL$$

The uniformly distributed load (p) to be applied is reported in Table 3.8-4 below:

Table 3.8-4

Uniformly Distributed Load (UDL)	
p	30 [kN/m]

The considered magnitude of the uniformly distributed load is comparable to the one adopted in the "S1600 stationary traffic load" paragraph of the Australian Standard for bridge design (Australian Standard 2017).

The variation "Δh" of the horizontal component of tension in the cable can be now evaluated according to Steinman's function B(k). The results obtained for uniformly distributed loads (p) applied from one end (point R) to a distance kL are reported in Table A3.7 in the Appendix and plotted in Figure 3.27 below:

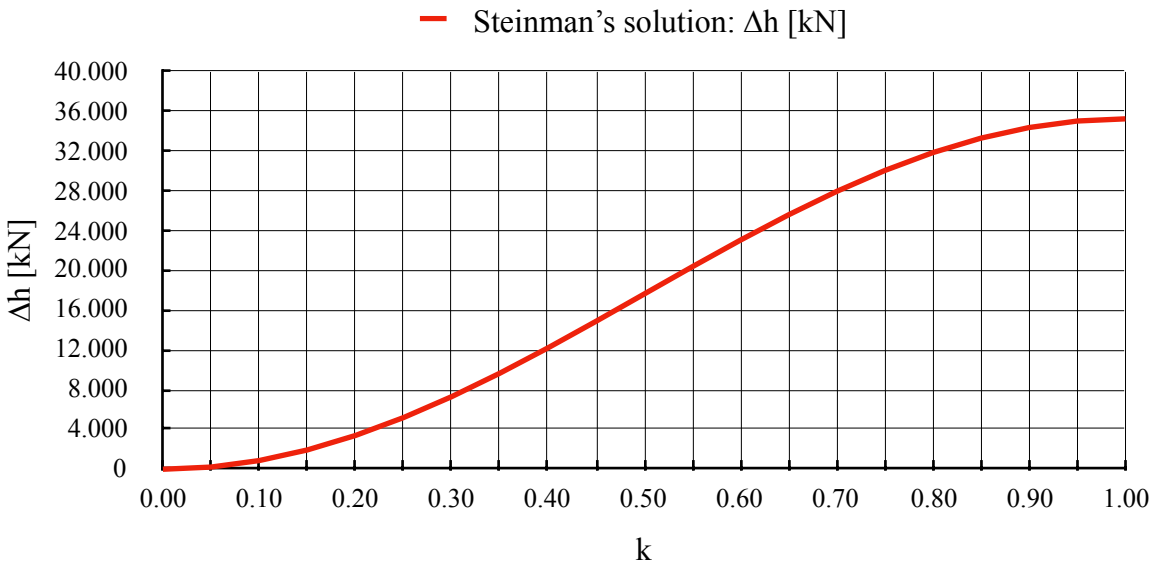

Figure 3.27: Steinman's solution, Δh due to UDL (p=30 kN/m).

The maximum variation Δh is found for a UDL (p) applied on the entire central span (k=1), its value and the correspondent variation of axial stress in the cable's central element are reported in Table 3.8-5 below:

Table 3.8-5

Maximum Δh	35,199 [kN]
Δσ	31.12 [MPa]

The obtained result shows that the most critical distributed load case would lead to an increase in the cable's diameter of 1.1% only. In particular:

$$A_m = \frac{\left[\left(\frac{g_{tot}}{2} + p\right)L_m + 2P\right]\sqrt{L_m^2 + 16k_m^2}}{8 f_{cbd} k_m - \gamma_{cb} L_m \sqrt{L_m^2 + 16k_m^2}}$$

Where:

$$\begin{cases} g = \frac{g_{tot}}{2} = 707.5 \text{ kN/m} \\ p = 30 \text{ kN/m} \\ P = 0 \text{ kN} \\ L_m = 960 \text{ m} \\ k_m = 97.83 \text{ m} \\ \gamma_{cb} = 77 \text{ kN/m}^3 \end{cases} \quad \Rightarrow \quad A_m = 1.309 \text{ m}^2$$

Hence the diameter:

$$D_m = \sqrt{\frac{4 \cdot A_m}{\pi}} = 1.291 \text{ m}$$

Hence the diameter's variation:

$$1 - \frac{1.277 \text{ m}}{1.291 \text{ m}} = 0.011 \quad \Rightarrow \quad 1.1\%$$

It is therefore demonstrated that the effect of distributed loads (Live Loads) is negligible in preliminary design.

C. Uniformly Distributed Load (p) Applied on all the Three Spans

It is also interesting to analyse the worst case scenario, even if this will not be compared to the corresponding Strand7 solution.

The worst case scenario for a uniformly distributed load is found when the entire length of the bridge is loaded. The variation of tension in the cable Δh is given by the following formula:

$$\Delta h_{\max} = \frac{L}{5Nd} \cdot \left(1 + 2 \frac{I \cdot L_1^3 \cdot d_1}{I_1 \cdot L^3 \cdot d} \right) pL$$

$$\Delta h_{\max} = 35{,}278 \text{ kN}$$

The correspondent variation of axial stress in the cable's central element is:

$$\Delta \sigma_{\max} = 31.19 \text{ MPa}$$

It is clear form the results obtained in cases B and C that extending the uniformly distributed load to the side spans does not provoke a large increase of tension in the main span cable (79 kN only).

3.8.2. Strand7 Solution

The load cases presented in the previous paragraph are also analysed with the software Strand7. As already reported in previous considerations the horizontal component of tension in the cable due to dead load only, according to Strand7, is:

$$H(G) = 222{,}892.3 \text{ kN}$$

The variation of this component due to the applied loads will be calculated as:

$$\Delta h = H(P(k) + G) - H(G)$$
$$\Delta h = H(p(k) + G) - H(G)$$

where:

- H(P(k)+G) is the horizontal component of tension in the cable due to dead load (G) and the applied point load (P(k));
- H(p(k)+G) is the horizontal component of tension in the cable due to dead load (G) and the applied UDL (p(k)).

The obtained results are presented below.

A. <u>Single load (P) Applied on the Main Span at a Distance kL from the Pylon (point R)</u>

The values obtained in Strand7 for this load case are reported in Table A3.8 in the Appendix and plotted in Figure 3.28 below:

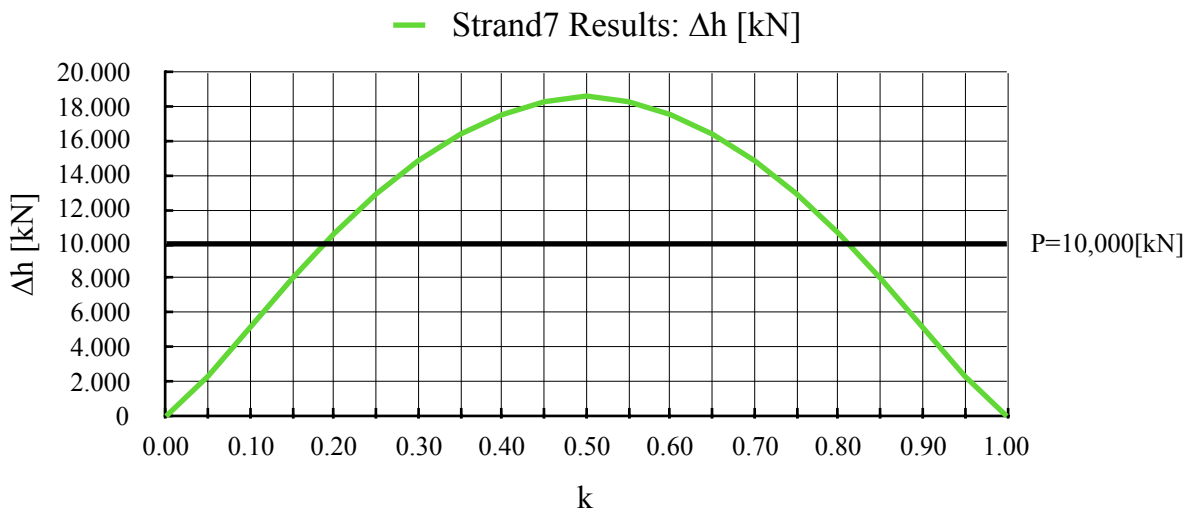

Figure 3.28: Strand7 results, Δh due to point load (P=10,000 kN).

The maximum variation Δh is found for a point load (P) applied at midspan (k=0.5), its value and the correspondent variation of axial stress in the cable's central element are reported in Table 3.8-6 below:

Table 3.8-6

Maximum Δh	18,600 [kN]
Δσ	16.45 [MPa]

B. <u>Uniformly Distributed Load (p) Applied from the Pylon (point R) to a Distance kL</u>

The values obtained in Strand7 for this load case are reported in Table A3.9 in the Appendix and plotted in Figure 3.29 below:

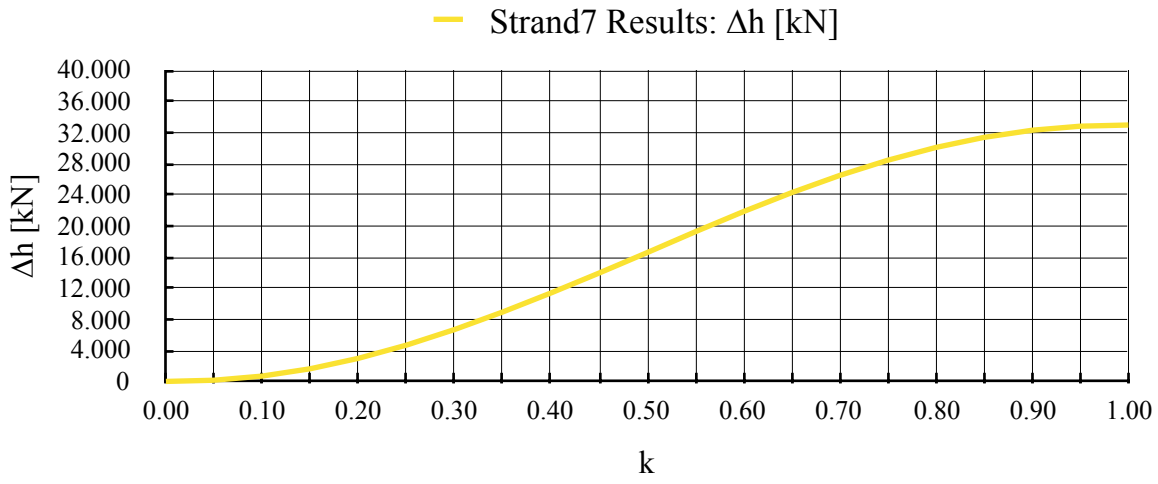

Figure 3.29: Strand7 results, Δh due to UDL (p=30 kN/m).

The maximum variation Δh is found for a UDL (p) applied on the entire central span (k=1), its value and the correspondent variation of axial stress in the cable's central element are reported

in Table 3.8-7 below:

Table 3.8-7

Maximum Δh	32,951 [kN]
Δσ	29.14 [MPa]

3.8.3. Analysis of Results

It is finally possible to compare software-based results with Steinman's solution. The obtained plots are assembled together and the discrepancy between results is reported in a graph showing the error percentage.

A. <u>Single load (P) Applied on the Main Span at a Distance kL from the Pylon (point R)</u>

Steinman's solution and Strand7 results for the variation of the horizontal component of tension in the cable are shown in Figure 3.30 below:

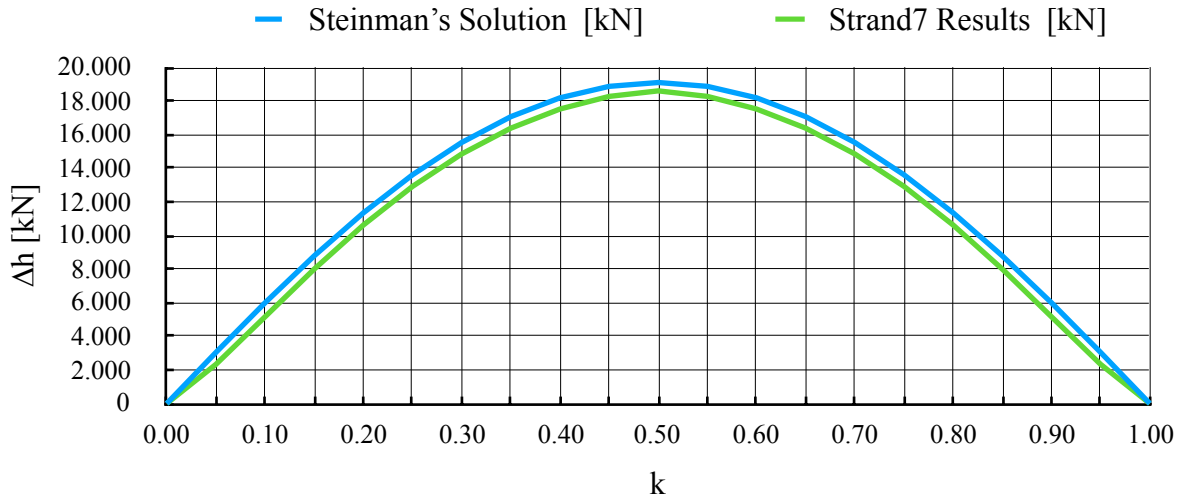

Figure 3.30: Comparing Steinman's solution with Strand7 results.

As noticeable from the obtained results, Steinman's solution provides more conservative results compared to Strand7. The discrepancy between the two, for different values of k, is reported in Figure 3.31 below:

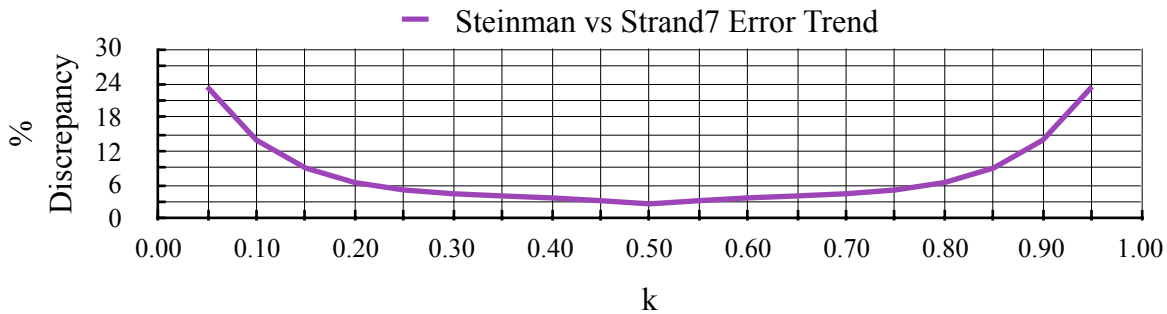

Figure 3.31: Discrepancy between Steinman's solution and Strand7 results.

It is clear that the accuracy of Steinman's solution for this particular load case is quite low for concentrated forces applied in proximity of the pylons' zone, where the main span supports are located. The maximum error is found for k=0.05 with a discrepancy of 23.36%. However, as the load's application point moves toward the centre of the span, the results' accuracy increases up to a minimum discrepancy of 2.60% for k=0.50. Table 3.8-8 below shows the maximum and minimum discrepancies in terms of horizontal component of tension in the cable Δh:

Table 3.8-8

k	Discrepancy (%)	Discrepancy (Δh)
0.05	23.36%	710.40 [kN]
0.50	2.60%	496.95 [kN]

All the results obtained for this load case are reported in the Appendix in Table A3.10.

B. <u>Uniformly Distributed Load (p) Applied from the Pylon (point R) to a Distance kL</u>

Steinman's solution and Strand7 results for the variation of the horizontal component of tension in the cable are shown in Figure 3.32 below:

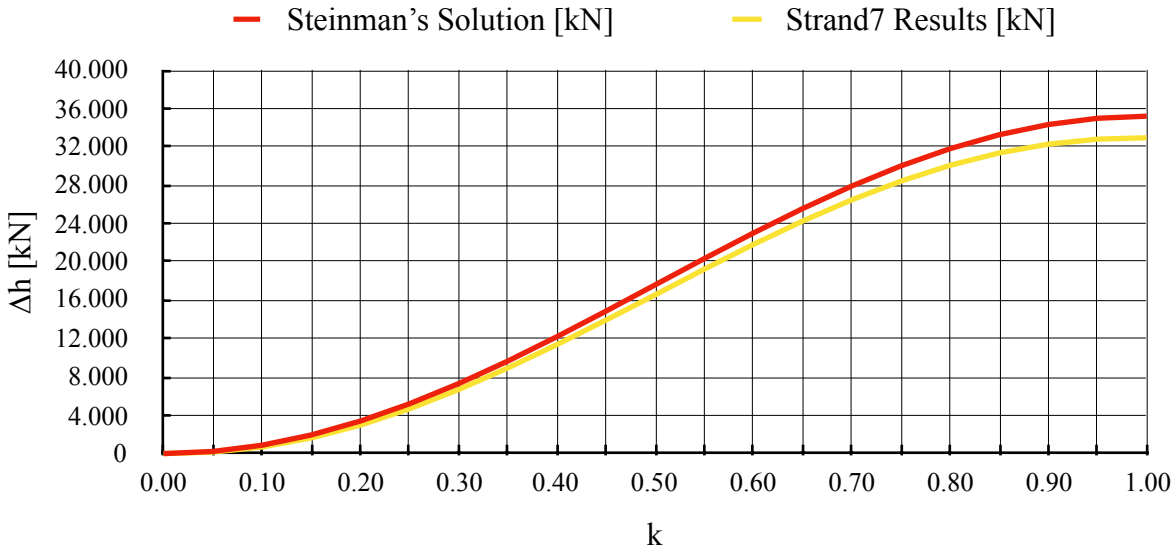

Figure 3.32: Comparing Steinman's solution with Strand7 results.

As noticeable from the obtained results, Steinman's solution provides more conservative results compared to Strand7. The discrepancy between the two, for different values of k, is reported in Figure 3.33. below:

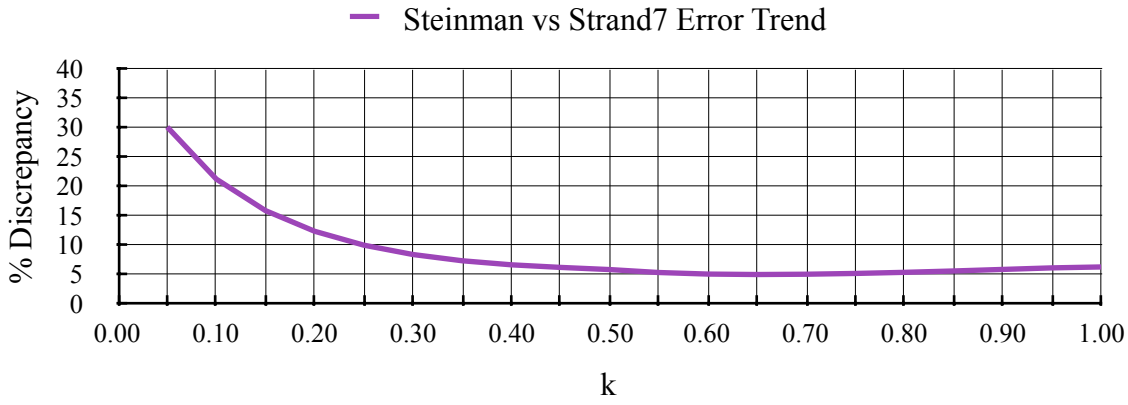

Figure 3.33: Discrepancy between Steinman's solution and Strand7 results.

The plotted results show that the accuracy of Steinman's solution increases with the value of k and therefore with the extension of the uniformly distributed load applied on the girder. The minimum discrepancy is obtained for k=0.65 (5.10%) whilst the maximum one for k=0.05 (30.19%). It is also noticeable that the discrepancy tends to increase for values of k larger than 0.65 but this variation is very small and does not exceed 7%.

Table 3.8-9 below shows the discrepancies in terms of horizontal component of tension in the cable Δh for the most relevant values of k:

Table 3.8-9

k	Discrepancy (%)	Discrepancy (Δh)
0.05	30.19%	66.26 [kN]
0.65	5.10%	1,303.48 [kN]
1.00	6.39%	2,248.32 [kN]

All the results obtained for this load case are reported in the Appendix in Table A3.11.

3.8.4. Final Considerations

The analysis conducted on Strand7 has shown that Steinman's functions can be usefully applied for determining the variation of the horizontal component of tension in the cable. Relevant discrepancies have been observed for particular types of load cases but in general terms Steinman's solution represents a reliable tool to be adopted in a preliminary design.

As a matter of fact, the plots and results reported in the previous paragraphs (the complete list of results is also reported in the Appendix) show that the discrepancy between Steinman's solution and Strand7 results decreases with increasing values of Δh. This means that as the load pattern becomes more critical, the result's accuracy increases.

It is duty-bound to inquire about the sources of error for the analysed results.

Discrepancies might be found in Steinman's hypotheses, in particular:

- *The initial horizontal component of tension in the cable H is constant along the entire length of the bridge (R_1-S_1)*
- *There is no bending action in the stiffening girder at this stage (dead load only)*

As already mentioned in paragraph 3.7.3 (Nonlinear static analysis), the Strand7 simulation shows that the horizontal component of tension in the cable due to dead load only is not constant. Moreover, Strand7 accounts for the initial bending action due to dead load in the stiffening girder.

The two mentioned hypothesis could therefore represent sources of error.

Furthermore, the freely hanging cable shape was not perfectly modelled due to time consuming issues related to Strand7 already explained in paragraph 3.5.2 (Main Suspension Cable). The cited approximation could therefore be one of the reasons for the discrepancies detected in the conducted analysis.

Moreover, the obtained results show that it is reasonable to neglect the contribution of Live Loads (distributed and concentrated loads) during preliminary design phases.

3.9. The Influence of Side Spans

The choice of the side span to main span ratio is generally driven by the characteristics of the construction site. For instance, long side span bridges are usually adopted in cases where all the three spans have to be placed on deep water. The use of long side spans leads to the design of side cables having a sag which is considerably larger compared to the one of a short side span bridge. As reported in "Cable supported Bridges" (Gimsing 1997) this design asset would therefore unfavourably influence the horizontal restraint of the pylon top. This implies that short side spans have a positive effect on the restraint of the pylon's top to horizontal movements. In fact, cables with smaller sags are characterised by a larger axial stiffness (Gimsing 1997).

It is therefore interesting to design a second model of the suspension bridge on Strand7, characterised by:

- The same main span length as the one of the model already analysed
- The same truss girder and pylon's properties (material and geometrical)
- Long side spans (span ration r_L in the range 0.4 - 0.5)

In these conditions, according to "Cable supported Bridges" (Gimsing 1997), it is therefore reasonable to expect a larger main span deflection and a larger pylon top displacement.

It is also assumed that, as the main span is the larger out of the three, its length is going rule the design of the truss girder. This assumption will be commented at the end of this analysis.

3.9.1. Long Side Spans Suspension Bridge - Design Parameters

The preliminary design procedure has already been reported in the previous paragraphs. The formulas to be adopted for a long side span suspension bridge are the same as those already presented. Thus, there is no need to fully report the procedure again. The main design parameters are reported below.

First of all, spans' proportions and lengths are redefined as reported in Table 3.9-1 below:

Table 3.9-1

Spans' Proportions and Lengths		
Span Ratio	r_L	0,50
Main Span Length	L_m	960 [m]
Side Span Length	$L_a = 0.50 \cdot L_m$	480 [m]
Total Length	$L_m + 2 \cdot L_a$	1920 [m]

Given the same material properties and girder geometry adopted for the short side span suspension bridge, the Dead Load is determined and reported in Table 3.9-2 below:

Table 3.9-2

Dead Load Determination - Self Weight Only
$g_{tot} = 1413$ kN/m

Note: in the performed calculation, half of the UDL has to be considered because there are two planes of cables supporting the bridge. Reference will thus be made to ($g_{tot}/2$):

$$\frac{g_{tot}}{2} = 706.5 \text{ kN/m}$$

The hangers' properties result unvaried as reported in Table 3.9-3 below:

Table 3.9-3

Hangers' Properties		
Central Hangers' Length	j_m	3 [m]
Hangers' Spacing	λ	15 [m]
Hangers' Diameter	D_h	0.150 [m]

The main span cable's properties result unvaried as well. The cable's shape is identical to the one defined for the short span suspension bridge. The only difference will be in the z-axis coordinates to be set in Strand7 as the main span is moved due to the change in the side span length. The relevant design parameters are reported in Table 3.9-4 below:

Table 3.9-4

Main Cable Properties		
Sag	k_m	97.83 [m]
Sag Ratio	$s_{r,m}$	0,102
Pylon Top (y) Coordinate	$H_{pt} = k_m + j_m$	100.83 [m]
Diameter	D_m	1.2 [m]
Cross-sectional Area	A_m	1.13 [m^2]
Weight of the Cable / Unit Length	μ_m	87.1 [kN/m]

The plot showing the nodes and the cable's profile (the right half of it) is schematically shown in Figure 3.34 below (not in scale):

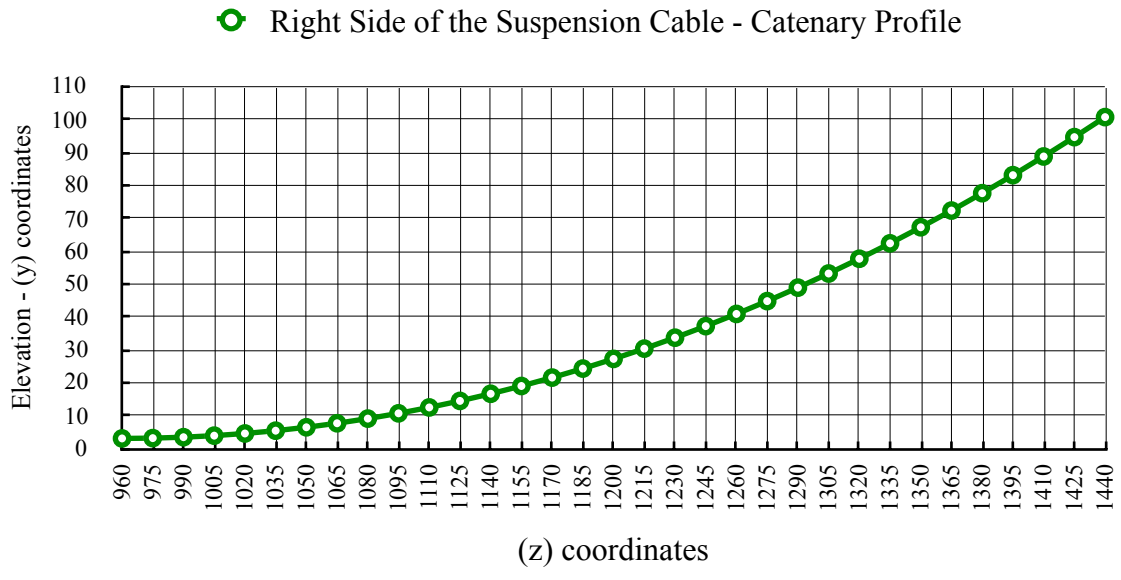

Figure 3.34: Catenary profile for the Strand7 model, long side spans model.

For the determination of the side cable sag, reference is made to the simplified expression reported in paragraph 3.5.3:

$$k_{a,simplified} = \frac{g_a + p_a}{g_m + p_m}\left(\frac{L_a}{L_m}\right)^2 \cdot k_m$$

As for the short side spans suspension bridge, the traffic load is initially ignored. The expression is therefore rewritten as:

$$k_{a,simplified} = \left(\frac{L_a}{L_m}\right)^2 \cdot k_m = 24.457 \text{ m}$$

The resulting sag ratio is therefore:

$$s_{r,a} = \frac{k_{a,simplified}}{L_a} = 0.051$$

Moreover, the quantity of cable steel for one side cable is calculated as:

$$Q_{ca,1} = 48,789 \text{ kN}$$

Given the side cable's free length $L_{a,f}$ the diameter is finally determined:

$$L_{a,f} \simeq 494.43 \text{ m}$$

$$D_a \simeq 1.3 \text{ m} \quad \Rightarrow \quad D_a = 1.2 \text{ m}$$

The relevant design parameters for the side cables are reported in Table 3.9-5 below:

Table 3.9-5

Side Cables Properties		
Sag	k_a	24.46 [m]
Sag Ratio	$s_{r,a}$	0,051
Diameter	D_a	1.2 [m]
Cross-sectional Area	A_a	1.13 [m^2]
Weight of the Cable / Unit Length	μ_a	87.1 [kN/m]

The plot showing the nodes and the profile of the right side cable is schematically shown in Figure 3.35 below (not in scale):

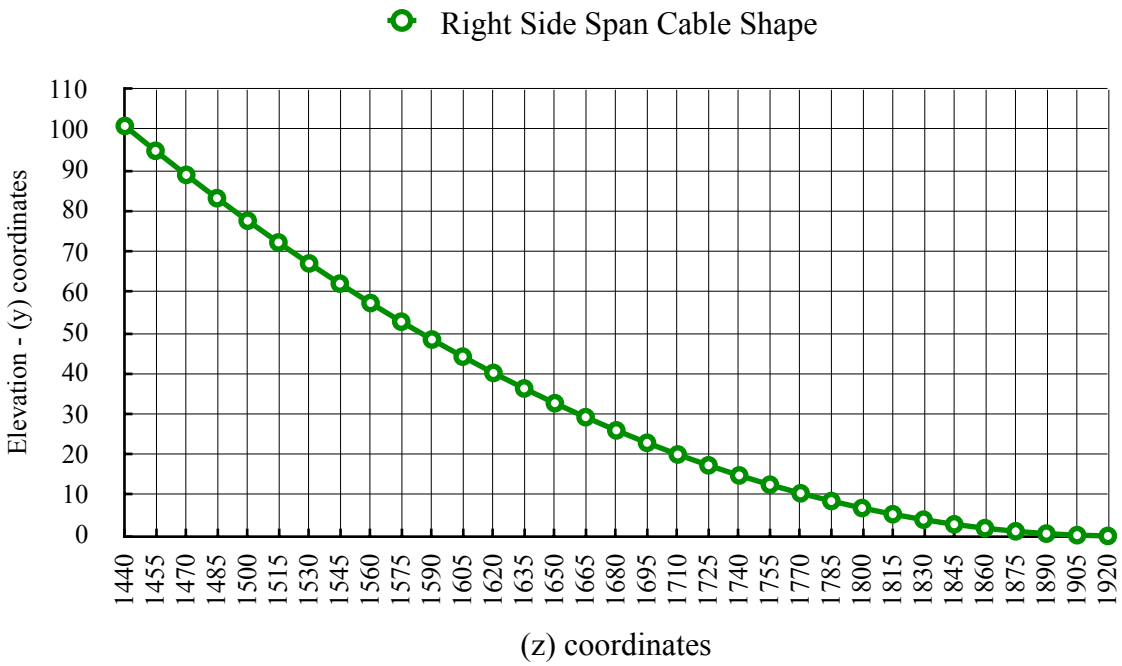

Figure 3.35: Catenary profile for the Strand7 model, long side spans model.

The coordinates of the side cable are reported in Table A3.12 in the Appendix.

3.9.2. Strand7 Simulation - Non-Linear Analysis

The model of the long side spans suspension bridge designed in Strand7 is shown in Figures 3.36 and 3.37 below:

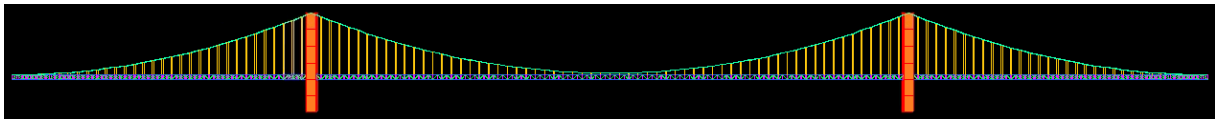

Figure 3.36: Strand7 model, YZ view (in scale).

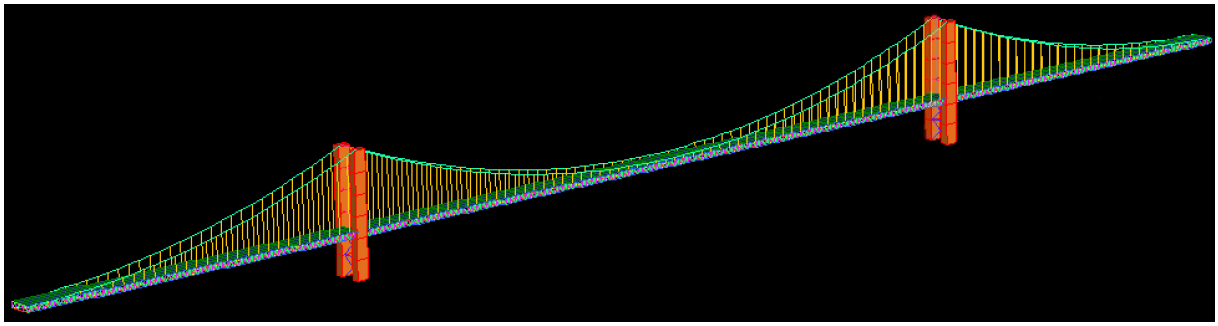

Figure 3.37: Strand7 model (in scale).

A series of interesting results is reported in Table 3.9-6 below, referring to Load Case 1 (G) where dead load only is considered:

Table 3.9-6

Nonlinear Static Analysis - Relevant Results for Nodes Displacements		
Result	**Node nº**	**Dimension**
Midspan Deflection δ_m	N. 238	- 1.99 [m]
Side Span Deflection δ_a	N. 190	- 3.87 [m]
Pylons' Top Displacement	N. 2577	Inward: 0.04 [m]

The correspondent deflection to span ratios will thus be:

$$\begin{cases} \dfrac{\delta_m}{L_m} = \dfrac{1.99}{960} \simeq \dfrac{1}{482} & \text{(main spam)} \\ \dfrac{\delta_a}{L_a} = \dfrac{3.87}{480} \simeq \dfrac{1}{124} & \text{(side spans)} \end{cases}$$

The horizontal component of tension in the cable elements and the correspondent axial stress are reported in Table 3.9-7 below:

Table 3.9-7

Nonlinear Static Analysis - Horizontal Component of Tension and Axial Stress			
Element Description	**Beam nº**	**H**	**σ**
Cable element at midspan	B. 6201	226,862.6 [kN]	200.59 [MPa]
Cable element at the pylon	B. 6359	227,311.0 [kN]	217.74 [MPa]
Side span central element	B. 6375	218,802.4 [kN]	198.59 [MPa]
Side span cable element at the pylon	B. 6360	218,972.2 [kN]	209.19 [MPa]

3.9.3. Comparing Long Span and Short Span Suspension Bridges

The obtained results show that there is a substantial difference between what it was expected according to Gimsing's text book and what Strand7 outputs. As a matter of fact the deflection of the main span (δ_m) and the pylon top displacement (δ_{Hp}) have been reduced, not increased:

$$\text{Short side spans bridge:} \quad \begin{cases} \delta_{m,s} = 2.37 \text{ m} \\ \delta_{Hp,s} = 0.12 \text{ m} \end{cases}$$

$$\text{Long side spans bridge:} \quad \begin{cases} \delta_{m,l} = 1.99 \text{ m} \\ \delta_{Hp,l} = 0.04 \text{ m} \end{cases}$$

The explanation to this phenomenon might be detected from the side spans' deflection. As reported in the tables above, the deflection of the side spans have considerably increased:

$$\text{Short side spans bridge:} \quad \delta_{a,s} = 0.71 \text{ m}$$
$$\text{Long side spans bridge:} \quad \delta_{a,l} = 3.87 \text{ m}$$

It is therefore clear that the larger deflection of the side span provokes a larger deflection in the side cables as well. This results in an increase of the horizontal action exerted by the side suspension cables on the pylon top towards the side spans. It therefore follows that the reduced pylon top displacement towards the main span also reduces the main span deflection.

However, the analysis given in "Cable supported Bridges" (Gimsing 1997) is not to be considered as unreasonable. In fact, the side spans deflection of the model used for the purpose of this research is too large. In order to reduce this deflection, a redesign of the side span portions of the truss girder should be considered.

This implies that even though the main span is characterised by the largest length, the effect of the side spans' length can not be neglected in the design of the truss girder.

4. Conclusions

An initial analysis on the structural behaviour of cables and on the main theories for suspension bridges have been carried out in order to acquire the knowledge and analytical tool required for the implementation of the case study. Preliminary design guidelines have been collected, analysed and put into practice for the design of a suspension bridge model in Strand7. Furthermore, software-based results have been compared to theoretical results obtained by the application of the Steinman's Modified Elastic Treatment to the case study.
The experience gained during the project and the analysis of the obtained results led to interesting conclusions.

First of all, it is fundamental to underline that the comparison between software-based and theoretical results proves that the simplified treatment proposed by Steinman provides reliable results. This allows Structural Engineers to rely on this method for a preliminary design and avoid time-consuming numerical methods in the initial phases of their study or project. It is although important to state that numerical methods provide a wider range of more precise results and should therefore be applied for a final design. However, this consideration does not discredit the Steinman Modified Elastic Treatment, which is meant to substitute numerical methods for the evaluation of a restricted range of results.

Second, the conducted research has shown that there is a lack of guidelines for the determination of the structural characteristics of the truss girder. The interaction between the stiffening girder and the cable system plays a fundamental role in the design of the structural elements composing the bridge. However, no refined or clear methods are reported for the evaluation of the required bending capacity of the girder. Further studies could therefore be implemented in order to evaluate and include appropriate design criteria for the determination of the girder's bending capacity in the available guidelines. This would consequently lead to an optimisation of the quantity of steel required for the design of both the cable system and the girder itself.

Finally, an analysis of the influence of the side spans' length on the structural behaviour of suspension bridges has been conducted. As reported in the relevant chapter (3.9), the obtained results are not in line with those reported in the theory. However, the source of this discrepancy has been identified and related to the lack of design criteria already mentioned

above, regarding the scarce amount of available information for the determination of the girder's bending capacity.

Recommendations for further Study

The conducted research project represents the basis for further study on the interaction between the stiffening girder and the cable system. The Strand7 model created for this project could be adopted for the evaluation of the spans' deflection given different design assets of the bridge. The obtained results could be adopted for the determination of design criteria aimed at the evaluation of the girder's bending capacity. However, it is important to remember that Strand7 is not user friendly when it comes to the design of the cable system: if the cable's diameter changes, the catenary profile adopted for the representation of the cable's nodes will change accordingly. The user would therefore have to modify the cable profile and reconnect every node with cutoff bar elements in order to create the final cable system.

5. Acknowledgments

I would finally like to thank all the people who helped me along my academic path.

First of all, my supervisor Professor Peter Ansourian of the University of Sydney, who supported me during the implementation of my Thesis and always provided helpful suggestions for the achievement of optimal results.

Many thanks to my Italian supervisor Prof. Ing. Stefano Silvestri of the University of Bologna, for the interest he has shown in my work and the valuable suggestions provided.

Much obliged for the opportunity my parents gave me. None of this would have ever been possible without their support, love and passionate encouragement.

A special thanks to my life partner Chiara, for the encouragement and love she has always given me.

References

A. J. S. Pippard, SJB 1968, The analysis of engineering structures, Edward Arnold ltd.

Bleich, H 1935, Die berechung verankerter hängebrücken, Julis Springer.

Castigliano, A 1879, Théoréme de l' équilibre des systèmes élastiques et ses applications, Elastic Stresses in Structures.

Gimsing, NJ 1997, Cable supported bridges, concept and design.

Godard, MT 1894, Recherches sur le calcul de la reesistance des tabliers des ponts suspendus.

Irvine, HM 1981, *Cable structures*, The MIT Press.

J.B. Johnson, CWB, F.F. Turneaure 1910, Theory and practice of modern framed strctures.

Maugh, LC 1964, Statically indeterminate structures, John Wiley and Sons.

Podolny, W 1971, Static analysis of cable-stayed bridges, University of Pittsburg.

Pugsley, SA 1968, The theory of suspension bridges, Edward Arnold Publishers ltd.

R.J. Atkinson, RVS On the problem of stiffened suspension bridges and its treatment by relaxation method.

Rankine, WJM 1858, A manual of applied mechanics.

Routh, EJ 1891, Treatise on analytical statics.

Standard, A 2017, *Bridge design*.

Steinman, DB 1922, A practica treatise on suspension bridges, John Wiley.

Timoshenko, S 1928, Steifigkeit von hängebrücken, the stiffness of suspension bridges.

Walter Podolny, JBS 1976, 'Construction and design of cable stayed bridges' in, John Wiley & Sons.

Appendix

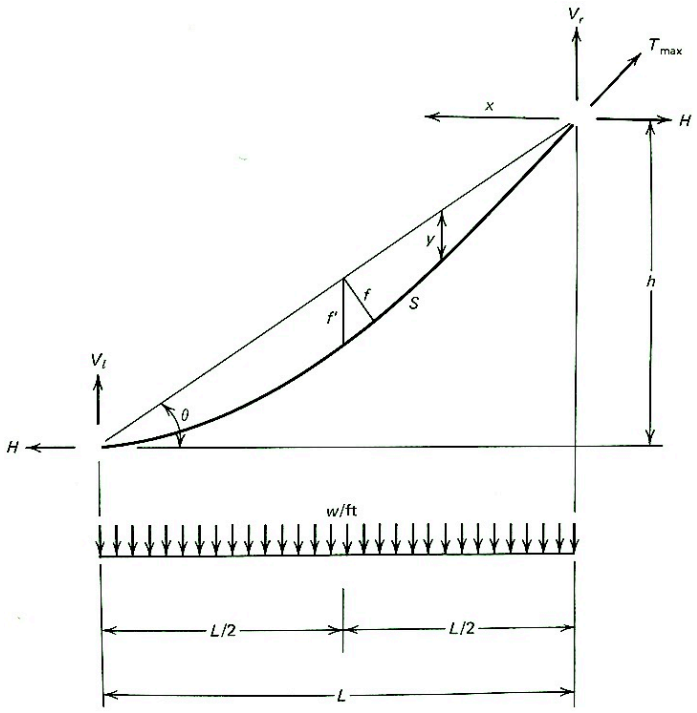

Figure A2.1: Cable with inclined chord (Walter Podolny 1976) .

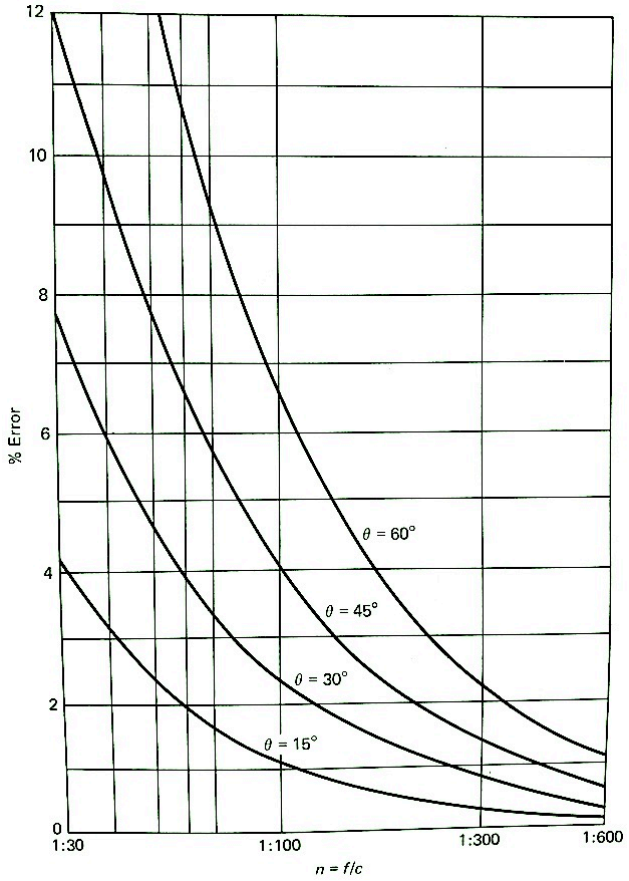

Figure A2.2: Percentage error of cable tension versus component along inclined chord (Walter Podolny 1976).

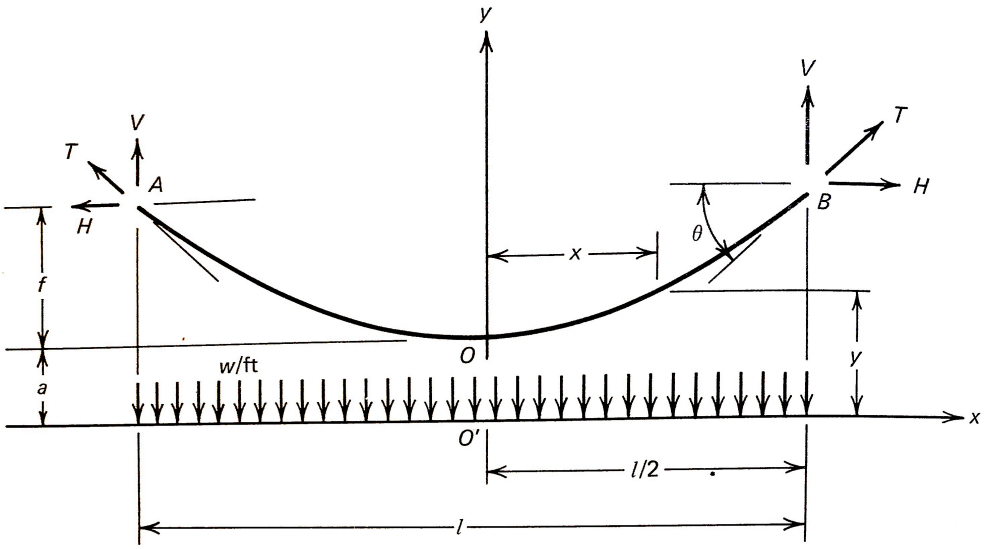

Figure A2.3: Nomenclature for cable's dimensions (Walter Podolny 1976).

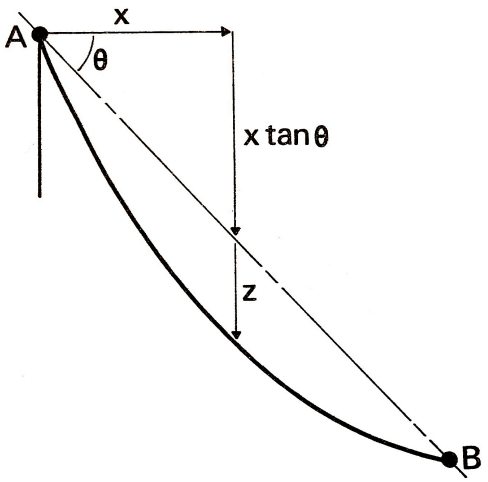

Figure A2.4: Definition diagram for an inclined cable (Irvine 1981).

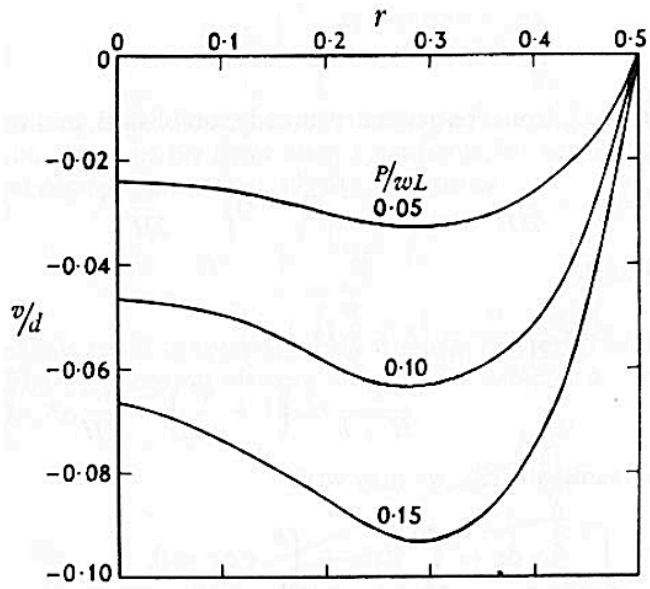

Figure A2.5: Variation of the deflection with (r) for different values of (P/wL) (Pugsley 1968).

TO VERTICAL LOADS
(unit load $P = 0{\cdot}1wL$)

Position of Load	Deflection (percentage of dip) at Station No.								
	1	2	3	4	5	6	7	8	9
1	− 5·28	− 2·95	− 1·07	+ 0·38	+ 1·40	+ 1·98	+ 2·13	+ 1·85	+ 1·15
2	− 2·95	− 6·65	− 3·15	− 0·38	+ 1·60	+ 2·81	+ 3·27	+ 2·94	+ 1·85
3	− 1·07	− 3·14	− 6·22	− 2·30	+ 0·60	+ 2·49	+ 3·38	+ 3·27	+ 2·13
4	+ 0·38	− 0·38	− 2·30	− 5·38	− 1·60	+ 1·02	+ 2·49	+ 2·81	+ 1·98
5	+ 1·40	+ 1·60	+ 0·60	− 1·60	− 5·00	− 1·60	+ 0·60	+ 1·60	+ 1·40
6	+ 1·98	+ 2·81	+ 2·49	+ 1·02	− 1·60	− 5·38	− 2·30	− 0·38	+ 0·38
7	+ 2·13	+ 3·27	+ 3·38	+ 2·49	+ 0·60	− 2·30	− 6·22	− 3·14	− 1·07
8	+ 1·85	+ 2·94	+ 3·27	+ 2·81	+ 1·60	− 0·38	− 3·15	− 6·65	− 2·95

Figure A2.6: Flexibility coefficients for vertical deflections due to vertical loads (unit load P=0.1wL) (Pugsley 1968).

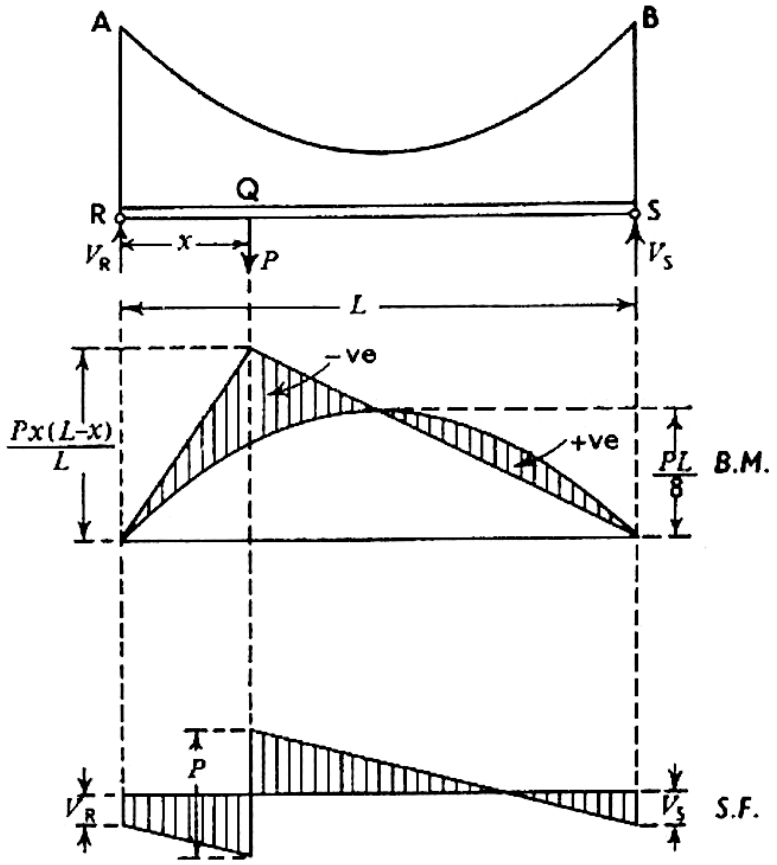

Figure A2.7: Bending Moment and Shear diagrams, Rankine Theory (Pugsley 1968).

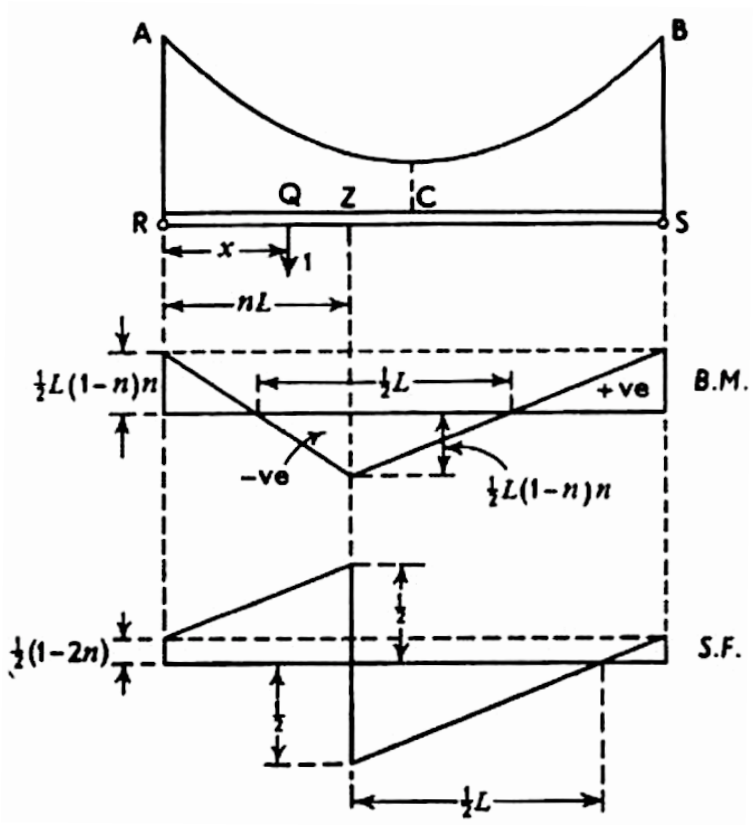

Figure A2.8: Influence lines for Bending Moment and Shear, Rankine Theory (Pugsley 1968).

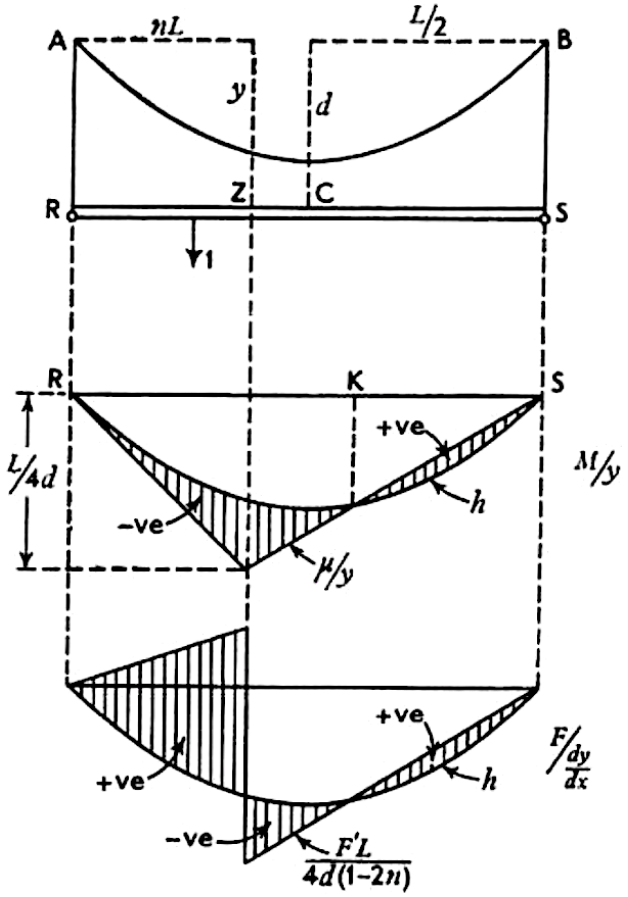

FigureA2.9 : Influence lines for (μ / y) and (h) (Pugsley 1968).

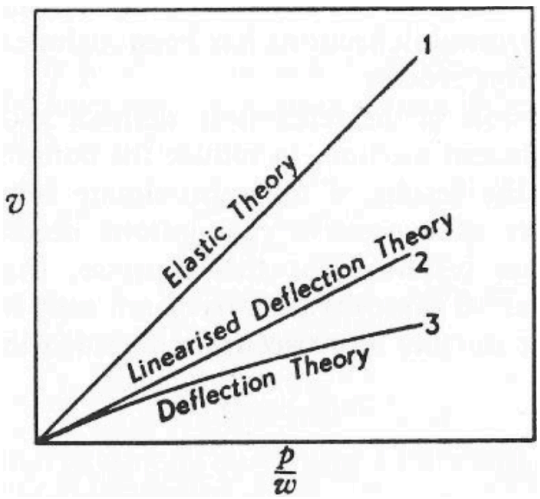

Figure A2.10: Comparison of Elastic, Deflection and Linearised Deflection Theories in terms of deflection (Pugsley 1968).

Table A3.1

Cable_1 Coordinates			
x	Catenary (y_c)	Parabola (y_p)	ABS(y_c - y_p)
0	0,0000	0,0000	0,00
15	0,2034	0,2263	0,02
30	0,8136	0,9052	0,09
45	1,8312	2,0368	0,21
60	3,2569	3,6209	0,36
75	5,0918	5,6577	0,57
90	7,3371	8,1471	0,81
105	9,9945	11,0891	1,09
120	13,0661	14,4838	1,42
135	16,5540	18,3310	1,78
150	20,4608	22,6309	2,17
165	24,7894	27,3834	2,59
180	29,5429	32,5885	3,05
195	34,7250	38,2462	3,52
210	40,3393	44,3566	4,02
225	46,3900	50,9195	4,53
240	52,8815	57,9351	5,05
255	59,8187	65,4033	5,58
270	67,2066	73,3241	6,12
285	75,0507	81,6976	6,65
300	83,3566	90,5236	7,17
315	92,1306	99,8023	7,67
330	101,3791	109,5336	8,15
345	111,1089	119,7175	8,61
360	121,3271	130,3540	9,03
375	132,0413	141,4432	9,40
390	143,2592	152,9849	9,73
405	154,9893	164,9793	9,99
420	167,2400	177,4263	10,19
435	180,0205	190,3259	10,31
450	193,3401	203,6782	10,34
465	207,2085	217,4830	10,27
480	221,6360	231,7405	10,10
495	236,6333	246,4506	9,82
510	252,2112	261,6133	9,40
525	268,3814	277,2286	8,85
540	285,1556	293,2966	8,14
555	302,5462	309,8171	7,27
570	320,5660	326,7903	6,22
585	339,2282	344,2161	4,99
600	358,5466	362,0945	3,55
615	378,5354	380,4255	1,89
630	399,2092	399,2092	0,00

Table A3.2

Cable_2 Coordinates			
x	Catenary (y_c)	Parabola (y_p)	ABS(y_c - y_p)
0	0,0000	0,0000	0,00
15	0,0847	0,0863	0,00
30	0,3387	0,3451	0,01
45	0,7622	0,7765	0,01
60	1,3551	1,3804	0,03
75	2,1175	2,1569	0,04
90	3,0495	3,1059	0,06
105	4,1513	4,2275	0,08
120	5,4230	5,5216	0,10
135	6,8647	6,9883	0,12
150	8,4766	8,6275	0,15
165	10,2590	10,4393	0,18
180	12,2121	12,4236	0,21
195	14,3360	14,5805	0,24
210	16,6311	16,9099	0,28
225	19,0978	19,4119	0,31
240	21,7362	22,0864	0,35
255	24,5467	24,9335	0,39
270	27,5297	27,9531	0,42
285	30,6856	31,1453	0,46
300	34,0147	34,5100	0,50
315	37,5175	38,0472	0,53
330	41,1945	41,7571	0,56
345	45,0461	45,6394	0,59
360	49,0727	49,6944	0,62
375	53,2750	53,9218	0,65
390	57,6534	58,3219	0,67
405	62,2085	62,8944	0,69
420	66,9410	67,6395	0,70
435	71,8513	72,5572	0,71
450	76,9401	77,6474	0,71
465	82,2080	82,9102	0,70
480	87,6558	88,3455	0,69
495	93,2842	93,9534	0,67
510	99,0938	99,7338	0,64
525	105,0853	105,6868	0,60
540	111,2596	111,8123	0,55
555	117,6175	118,1104	0,49
570	124,1597	124,5810	0,42
585	130,8871	131,2242	0,34
600	137,8005	138,0399	0,24
615	144,9008	145,0282	0,13
630	152,1890	152,1890	0,00

Table A3.3

Main Cable - Strand7 Coordinates - Catenary Profile		
x Strand7	y Strand7	z Strand7
0,00	3,00	720
0,00	3,09	735
0,00	3,38	750
0,00	3,85	765
0,00	4,51	780
0,00	5,36	795
0,00	6,39	810
0,00	7,62	825
0,00	9,04	840
0,00	10,64	855
0,00	12,44	870
0,00	14,42	885
0,00	16,60	900
0,00	18,96	915
0,00	21,52	930
0,00	24,27	945
0,00	27,21	960
0,00	30,34	975
0,00	33,67	990
0,00	37,19	1005
0,00	40,90	1020
0,00	44,81	1035
0,00	48,91	1050
0,00	53,21	1065
0,00	57,71	1080
0,00	62,40	1095
0,00	67,29	1110
0,00	72,38	1125
0,00	77,66	1140
0,00	83,15	1155
0,00	88,84	1170
0,00	94,73	1185
0,00	100,83	1200

Table A3.4

Right Side Span - Cable Coordinates				
y_C (Inclined Chord)	y_D (Distance)	x Strand7	y Strand7	z Strand7
100,83	0,00	0,00	100,83	1200
94,53	5,63	0,00	88,90	1215
88,22	10,50	0,00	77,72	1230
81,92	14,63	0,00	67,30	1245
75,62	18,00	0,00	57,62	1260
69,32	20,63	0,00	48,69	1275
63,02	22,50	0,00	40,52	1290
56,72	23,63	0,00	33,09	1305
50,41	24,00	0,00	26,41	1320
44,11	23,63	0,00	20,49	1335
37,81	22,50	0,00	15,31	1350
31,51	20,63	0,00	10,88	1365
25,21	18,00	0,00	7,21	1380
18,91	14,63	0,00	4,28	1395
12,60	10,50	0,00	2,10	1410
6,30	5,63	0,00	0,68	1425
0,00	0,00	0,00	0,00	1440

Table A3.5

Steinman's Functions for Applications of Elastic Theory					
k	B(k)	C(k)	D(k)	F(k)	G(k)
0,00	0,0000	0,00000	2,0000	0,0000	0,4000
0,05	0,0498	0,05238	1,7576	0,0062	0,4405
0,10	0,0981	0,10900	1,5309	0,0248	0,4816
0,15	0,1438	0,16913	1,3204	0,0551	0,5232
0,20	0,1856	0,23200	1,1264	0,0963	0,5648
0,25	0,2227	0,29688	0,9492	0,1475	0,6063
0,30	0,2541	0,36300	0,7889	0,2072	0,6472
0,35	0,2793	0,42963	0,6454	0,2740	0,6874
0,40	0,2976	0,49600	0,5184	0,3462	0,7264
0,45	0,3088	0,56138	0,4076	0,4222	0,7641
0,50	0,3125	0,62500	0,3125	0,5000	0,8000
0,55	0,3088	0,68613	0,2324	0,5778	0,8340
0,60	0,2976	0,74400	0,1664	0,6538	0,8656
0,65	0,2793	0,79788	0,1136	0,7260	0,8947
0,70	0,2541	0,84700	0,0729	0,7928	0,9208
0,75	0,2227	0,89063	0,0430	0,8525	0,9438
0,80	0,1856	0,92800	0,0224	0,9037	0,9632
0,85	0,1438	0,95838	0,0096	0,9449	0,9789
0,90	0,0981	0,98100	0,0029	0,9752	0,9904
0,95	0,0498	0,99513	0,0004	0,9938	0,9976
1,00	0,0000	1,00000	0,0000	1,0000	1,0000

Table A3.6

Steinman's solution for Applied Point Loads		
k	kL [m]	Δh [kN]
0,00	0,00	0
0,05	48,00	3.041
0,10	96,00	5.995
0,15	144,00	8.785
0,20	192,00	11.342
0,25	240,00	13.607
0,30	288,00	15.528
0,35	336,00	17.065
0,40	384,00	18.186
0,45	432,00	18.868
0,50	480,00	19.097
0,55	528,00	18.868
0,60	576,00	18.186
0,65	624,00	17.065
0,70	672,00	15.528
0,75	720,00	13.607
0,80	768,00	11.342
0,85	816,00	8.785
0,90	864,00	5.995
0,95	912,00	3.041
1,00	960,00	0
Applied Load	P	10000 [kN]

Table A3.7

Steinman's solution for Uniformly Distributed Loads		
k	kL [m]	Δh [kN]
0,00	0,00	0
0,05	48,00	219
0,10	96,00	872
0,15	144,00	1.938
0,20	192,00	3.390
0,25	240,00	5.191
0,30	288,00	7.293
0,35	336,00	9.644
0,40	384,00	12.187
0,45	432,00	14.861
0,50	480,00	17.600
0,55	528,00	20.339
0,60	576,00	23.012
0,65	624,00	25.555
0,70	672,00	27.907
0,75	720,00	30.009
0,80	768,00	31.809
0,85	816,00	33.261
0,90	864,00	34.328
0,95	912,00	34.980
1,00	960,00	35.199
UDL	p	30 [kN/m]

Table A3.8

Strand7 Results for Applied Point Loads			
k	H(G) [kN]	H(G+P(k)) [kN]	Δh [kN]
0,00	222.892,3	222.892	0
0,05	222.892,3	225.223	2.330
0,10	222.892,3	228.053	5.161
0,15	222.892,3	230.890	7.997
0,20	222.892,3	233.510	10.618
0,25	222.892,3	235.809	12.917
0,30	222.892,3	237.737	14.845
0,35	222.892,3	239.273	16.381
0,40	222.892,3	240.412	17.520
0,45	222.892,3	241.163	18.270
0,50	222.892,3	241.492	18.600
0,55	222.892,3	241.163	18.270
0,60	222.892,3	240.412	17.520
0,65	222.892,3	239.273	16.381
0,70	222.892,3	237.737	14.845
0,75	222.892,3	235.809	12.917
0,80	222.892,3	233.510	10.618
0,85	222.892,3	230.890	7.997
0,90	222.892,3	228.053	5.161
0,95	222.892,3	225.223	2.330
1,00	222.892,3	222.892	0
Applied Load P		P	10000 [kN]

Table A3.9

Strand7 Results for Applied UDL			
k	H(G) [kN]	H(G+p(k)) [kN]	Δh [kN]
0,00	222.892,3	222.892	0
0,05	222.892,3	223.046	153
0,10	222.892,3	223.578	686
0,15	222.892,3	224.521	1.629
0,20	222.892,3	225.860	2.968
0,25	222.892,3	227.559	4.667
0,30	222.892,3	229.565	6.673
0,35	222.892,3	231.819	8.927
0,40	222.892,3	234.257	11.365
0,45	222.892,3	236.815	13.923
0,50	222.892,3	239.446	16.554
0,55	222.892,3	242.124	19.232
0,60	222.892,3	244.713	21.821
0,65	222.892,3	247.144	24.252
0,70	222.892,3	249.362	26.469
0,75	222.892,3	251.316	28.423
0,80	222.892,3	252.961	30.068
0,85	222.892,3	254.256	31.364
0,90	222.892,3	255.172	32.279
0,95	222.892,3	255.692	32.800
1,00	222.892,3	255.843	32.951
Applied Load p		p	30 [kN/m]

Table A3.10

Steinman vs Strand7 Results for the Applied Point Loads				
k	Steinman's Δh [kN]	Strand7 Δh [kN]	% Error	Discrepancy [kN]
0,00	0	0	/	/
0,05	3.041	2.330	23,36%	710,40
0,10	5.995	5.161	13,91%	833,88
0,15	8.785	7.997	8,97%	787,73
0,20	11.342	10.618	6,38%	724,10
0,25	13.607	12.917	5,07%	689,81
0,30	15.528	14.845	4,40%	683,13
0,35	17.065	16.381	4,01%	684,33
0,40	18.186	17.520	3,66%	666,41
0,45	18.868	18.270	3,17%	597,87
0,50	19.097	18.600	2,60%	496,95
0,55	18.868	18.270	3,17%	597,87
0,60	18.186	17.520	3,66%	666,41
0,65	17.065	16.381	4,01%	684,33
0,70	15.528	14.845	4,40%	683,13
0,75	13.607	12.917	5,07%	689,81
0,80	11.342	10.618	6,38%	724,10
0,85	8.785	7.997	8,97%	787,73
0,90	5.995	5.161	13,91%	833,88
0,95	3.041	2.330	23,36%	710,40
1,00	0	0	/	/
Applied Load P			P	10000 [kN]

Table A3.11

Steinman vs Strand7 Results for the Applied UDL				
k	Steinman's Δh [kN]	Strand7 Δh [kN]	% Error	Discrepancy [kN]
0	0,00	0,00	/	
0,05	219,46	153,20	30,19%	66,26
0,1	871,54	685,70	21,32%	185,84
0,15	1938,09	1628,60	15,97%	309,49
0,2	3390,40	2968,10	12,46%	422,30
0,25	5190,52	4666,60	10,09%	523,92
0,3	7292,59	6672,60	8,50%	619,99
0,35	9644,14	8926,50	7,44%	717,64
0,4	12187,41	11364,50	6,75%	822,91
0,45	14860,70	13922,70	6,31%	938,00
0,5	17599,66	16553,50	5,94%	1046,16
0,55	20338,62	19231,70	5,44%	1106,92
0,6	23011,91	21820,60	5,18%	1191,31
0,65	25555,18	24251,70	5,10%	1303,48
0,7	27906,72	26469,20	5,15%	1437,52
0,75	30008,79	28423,30	5,28%	1585,49
0,8	31808,92	30068,40	5,47%	1740,52
0,85	33261,23	31364,10	5,70%	1897,13
0,9	34327,78	32279,20	5,97%	2048,58
0,95	34979,86	32800,10	6,23%	2179,76
1	35199,32	32951,00	6,39%	2248,32
Applied Load p			p	30 [kN/m]

Table A3.4-1

Right Side Span - Cable Coordinates for the Long Side Spans Suspension Bridge				
y_C (Inclined Chord)	y_D (Distance)	x Strand7	y Strand7	z Strand7
100,83	0,00	0,00	100,83	1440
97,68	2,96	0,00	94,72	1455
94,53	5,73	0,00	88,79	1470
91,37	8,31	0,00	83,06	1485
88,22	10,70	0,00	77,52	1500
85,07	12,90	0,00	72,18	1515
81,92	14,90	0,00	67,02	1530
78,77	16,72	0,00	62,05	1545
75,62	18,34	0,00	57,28	1560
72,47	19,78	0,00	52,69	1575
69,32	21,02	0,00	48,30	1590
66,17	22,07	0,00	44,10	1605
63,02	22,93	0,00	40,09	1620
59,87	23,60	0,00	36,27	1635
56,72	24,07	0,00	32,64	1650
53,56	24,36	0,00	29,20	1665
50,41	24,46	0,00	25,96	1680
47,26	24,36	0,00	22,90	1695
44,11	24,07	0,00	20,04	1710
40,96	23,60	0,00	17,36	1725
37,81	22,93	0,00	14,88	1740
34,66	22,07	0,00	12,59	1755
31,51	21,02	0,00	10,49	1770
28,36	19,78	0,00	8,58	1785
25,21	18,34	0,00	6,86	1800
22,06	16,72	0,00	5,34	1815
18,91	14,90	0,00	4,00	1830
15,75	12,90	0,00	2,86	1845
12,60	10,70	0,00	1,90	1860
9,45	8,31	0,00	1,14	1875
6,30	5,73	0,00	0,57	1890
3,15	2,96	0,00	0,19	1905
0,00	0,00	0,00	0,00	1920